



Measurement of $B^0_s \rightarrow \pi^0\pi^0$ at CEPC

Yuxin Wang, Manqi Ruan

CEPC Workshop, November 11, 2021

Outline

- 1. Motivation**
- 2. Separation of B^0 and B^0_s**
- 3. Event selection**
- 4. Dependence on b-tagging performance**
- 5. Dependence on B mass resolution**
- 6. Summary**

Motivation

From **physics aspect**

- **$B^0 \rightarrow \pi^0 \pi^0$ combined with $B^0 \rightarrow \pi^+ \pi^-$ and $B^+ \rightarrow \pi^+ \pi^0$, golden channels to determine the CKM angle: α (Φ_2)**
- “ **$B \rightarrow \pi\pi$ puzzle**”, the measured branching ratio of the $B^0 \rightarrow \pi^0 \pi^0$ is significantly larger than the theoretical predictions.
- **$B_s^0 \rightarrow \pi^0 \pi^0$, a pure annihilation process, $BR \sim 10^{-7}$, has not been observed.**
- **Tera-Z at CEPC with $10^{11} B^0$ and $10^{10} B_s^0$, at least 1-2 orders larger than Belle-II**

Modes	DATA [1]	SCET [2]	QCDF	pQCD
$B^+ \rightarrow \pi^+ \pi^0$	5.5 ± 0.4	5.20 ± 2.71	$6.00^{+3.76}_{-3.07}$	$4.27^{+1.85}_{-1.47}$
$B^0 \rightarrow \pi^+ \pi^-$	5.12 ± 0.19	5.40 ± 1.95	$8.90^{+5.55}_{-4.71}$	$7.67^{+3.27}_{-2.67}$
$B^0 \rightarrow \pi^0 \pi^0$	1.59 ± 0.26	0.84 ± 0.46	$0.30^{+0.46}_{-0.26}$	$0.24^{+0.09}_{-0.07}$
$B_s^0 \rightarrow \pi^+ \pi^-$	0.7 ± 0.1	-	$0.26^{+0.10}_{-0.09}$	$0.52^{+0.21}_{-0.18}$
$B_s^0 \rightarrow \pi^0 \pi^0$	< 210	-	$0.13^{+0.05}_{-0.05}$	$0.21^{+0.10}_{-0.09}$

Table 1: Experimental measurements and theoretical predictions of the branching ratios (in unit of 10^{-6}) of $B \rightarrow \pi\pi$ system. The soft collinear effective theory (SCET), QCD factorization (QCDF), and perturbative QCD (pQCD) are three common theoretical techniques to deal with the hadronic B-meson decays.

From **detector aspect**

Clear dependence on the detector performance

- **b-tagging**
- **ECAL performance**

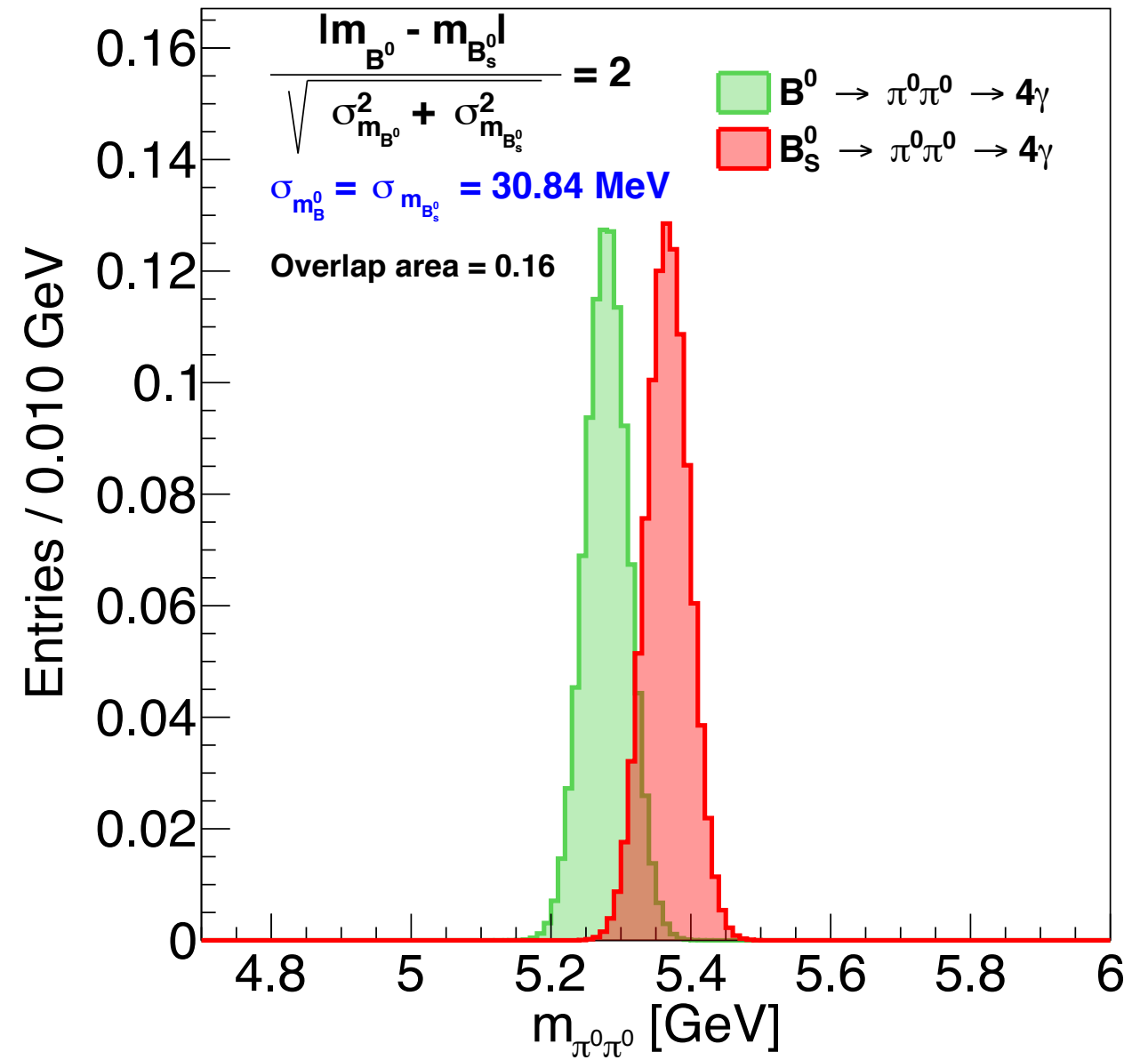
A Fast Simulation Analysis

Separation of B^0 and B_s^0

B meson mass

m_{B^0}	5279.65 ± 0.12 MeV
$m_{B_s^0}$	5366.88 ± 0.14 MeV
$m_{B_s^0} - m_{B^0}$	87.38 ± 0.16 MeV

$$\text{separation power} = \frac{|\bar{m}_{B^0} - \bar{m}_{B_s^0}|}{\sqrt{\sigma_{m_{B^0}}^2 + \sigma_{m_{B_s^0}}^2}}$$

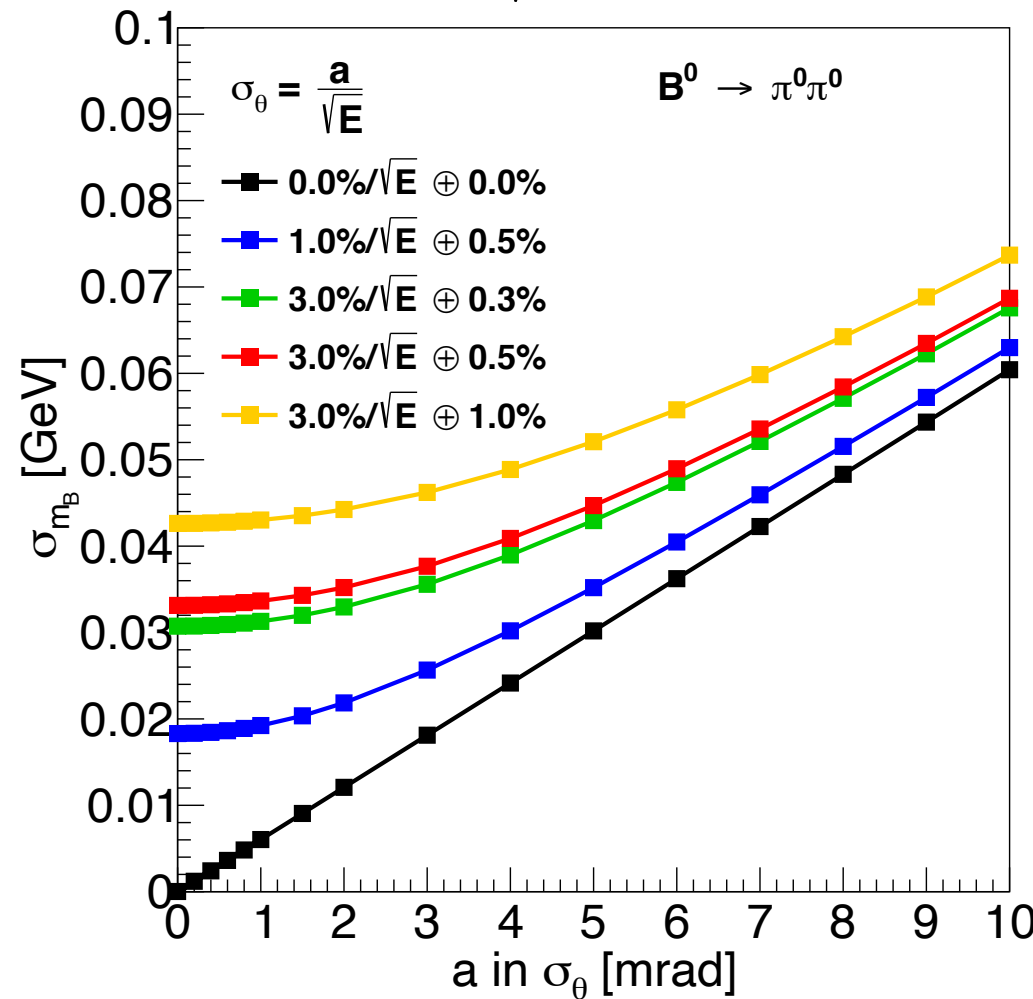


2 σ separation requires B mass resolution σ_{m_B} better than 30 MeV.

Dependence of B mass resolution on detector performance

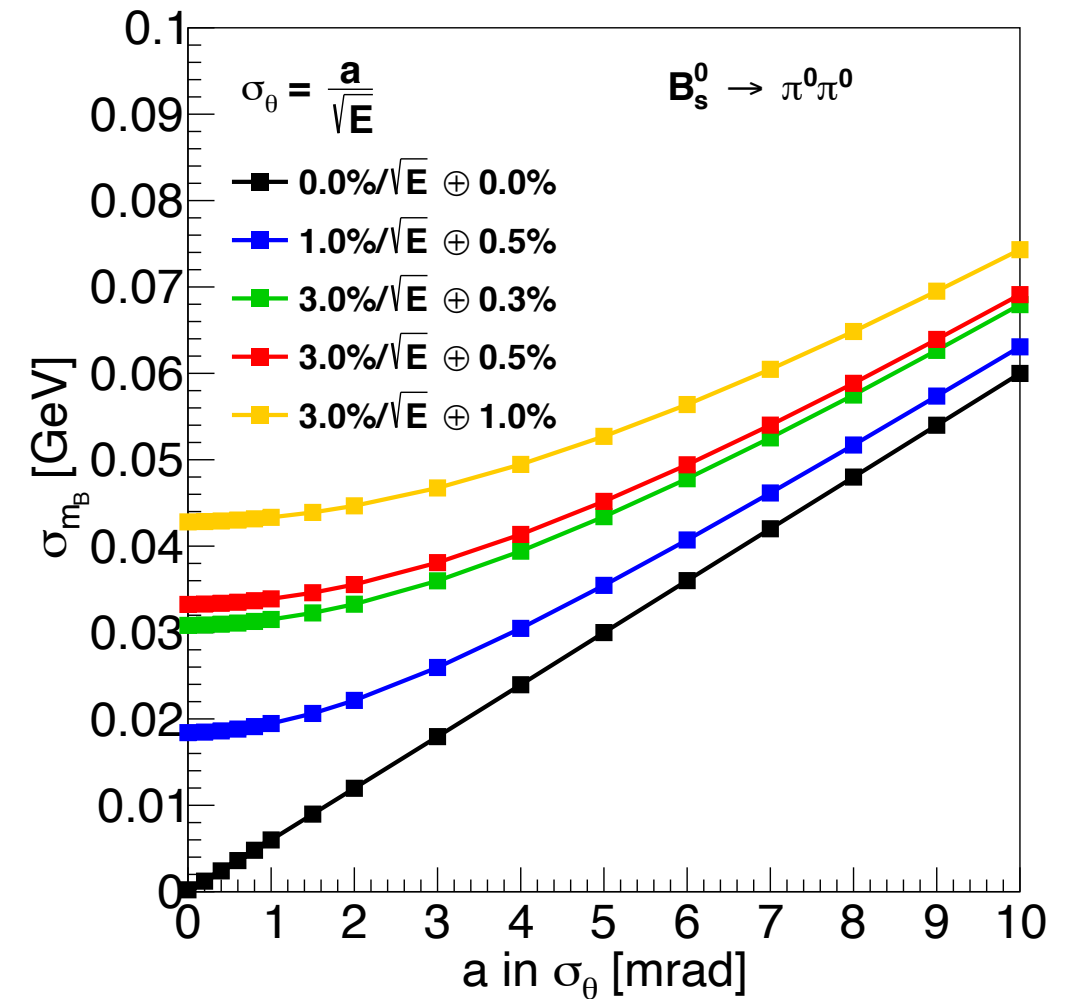
ECAL energy resolution

$$\frac{\sigma_E}{E} = \frac{A}{\sqrt{E}} \oplus C$$



Photon angular resolution

$$\sigma_\theta = \frac{a}{\sqrt{E}}, \quad \sigma_\phi = \frac{\sigma_\theta}{\sin\theta}$$

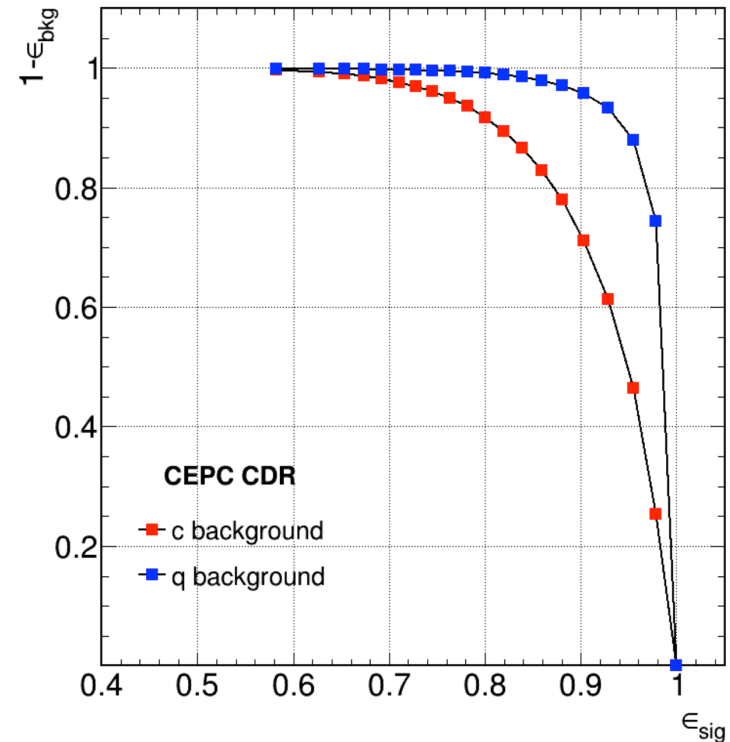


- CEPC baseline single photon angular resolution $\sim 1\text{mrad}/\sqrt{E}$
- ECAL energy resolution dominates the contribution when $\sigma_\theta < 1\text{mrad}/\sqrt{E}$
- The following analysis only takes ECAL energy resolution into account
- $\sigma_{m_B} \sim 30 \text{ MeV}$ requires ECAL energy resolution $\sim 3\%/\sqrt{E} \oplus 0.3\%$

Event Selection

CEPC baseline b-tagging

80% efficiency and 90% purity



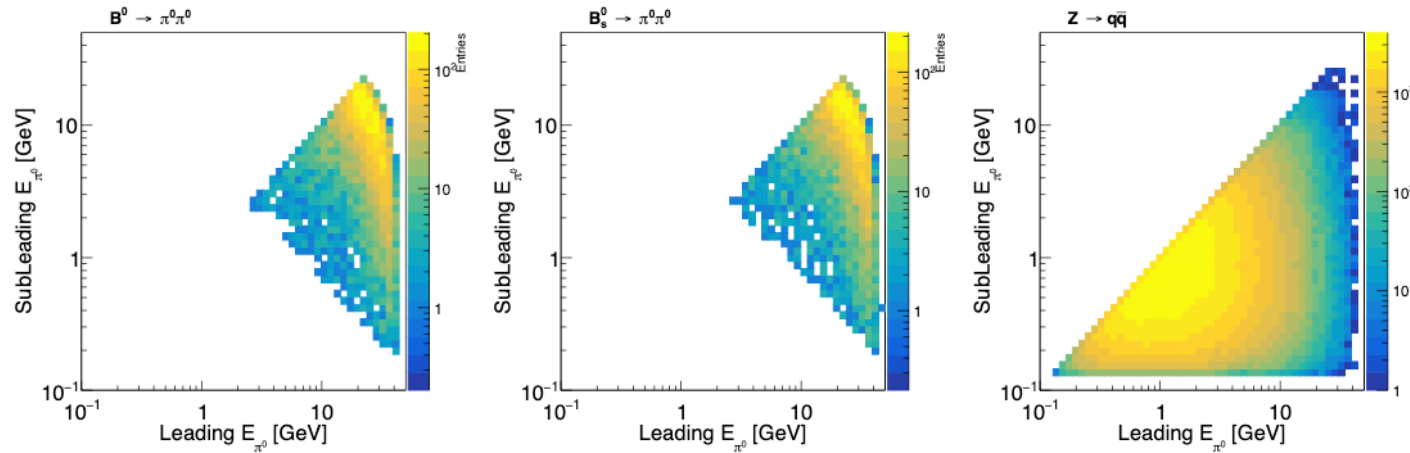
Numerical values used to estimate the signal statistics at Tera-Z.

$f(b \rightarrow B^0)$	0.407 ± 0.007
$f(b \rightarrow B_s^0)$	0.101 ± 0.008
$Br(B^0 \rightarrow \pi^0\pi^0)$	1.59×10^{-6}
$Br(B_s^0 \rightarrow \pi^0\pi^0)$	3×10^{-7}
$Br(\pi^0 \rightarrow \gamma\gamma)$	SM prediction
	98.823%

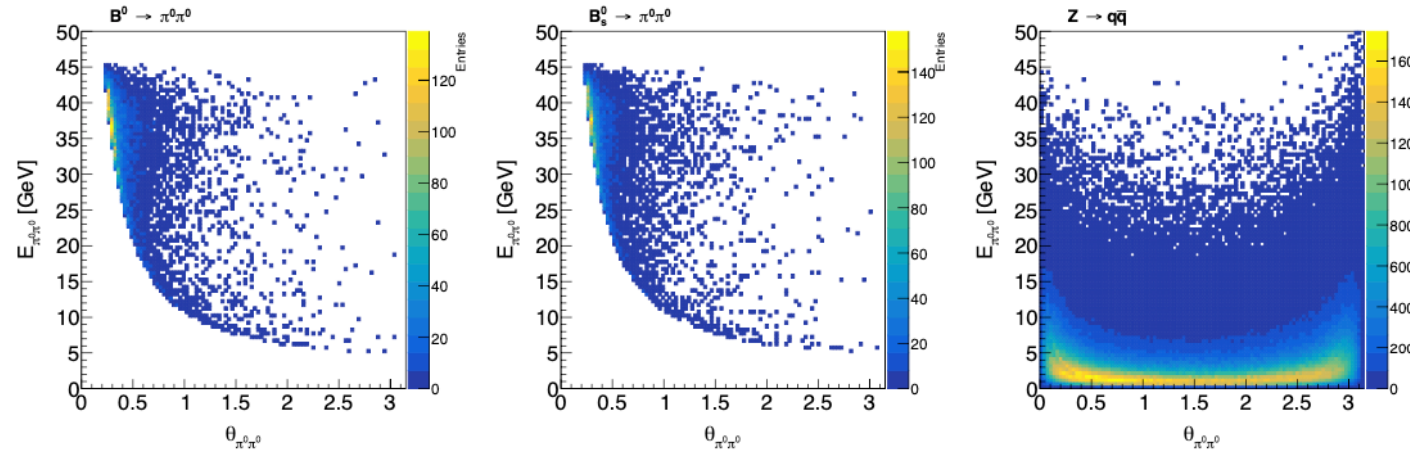
Cut chain table at 3%/ \sqrt{E} ⊕0.3% & CEPC baseline b-tagging

Cut chain	$B^0 \rightarrow \pi^0\pi^0$	$B_s^0 \rightarrow \pi^0\pi^0$	$q\bar{q}$	$u\bar{u} + d\bar{d} + s\bar{s}$	$c\bar{c}$	$b\bar{b}$	$\sqrt{S} + B/S$
Total generated	191113	8948	7e11 (100.00%)	4.285e11 (61.21%)	1.203e11 (17.19%)	1.512e11 (21.60%)	
b-tagging $(\epsilon_{b,c,uds \rightarrow b} = 80\%, 8.26\%, 0.85\%)$	152890	7158	1.34539e11 (100.00%)	3.64225e9 (2.70%)	9.93678e9 (7.38%)	1.2096e11 (89.92%)	
$\pi^0 \rightarrow \gamma\gamma$	147932	6959	134272699126	3605151069	9908563142	120758984915	
Lower $E_{\pi^0} > 6$ GeV	92172	4396	15490570779	843830534	1598643569	13048096676	
Higher $E_{\pi^0} > 14$ GeV	87057	4148	2534286670	307734259	314762436	1911789975	
$E_{\pi^0\pi^0} > 22$ GeV	86807	4133	2233308564	289771547	281656846	1661880170	
$\theta_{\pi^0\pi^0} < 23^\circ$	77626	3644	825367542	119076559	102055313	604235671	
$m_{\pi^0\pi^0} \in (5.2188, 5.3405) \text{ GeV}$ ($2.0 \sigma_{m_{B^0}} = 2.0 \times 0.0304 \text{ GeV}$)	75374	717	17896	5640	1656	10600	0.4067% ± 0.0106%
$m_{\pi^0\pi^0} \in (5.3421, 5.3917) \text{ GeV}$ ($0.8 \sigma_{m_{B_s^0}} = 0.8 \times 0.0310 \text{ GeV}$)	3769	2394	5477	2400	507	2570	4.5070% ± 0.5563%

Event Selection



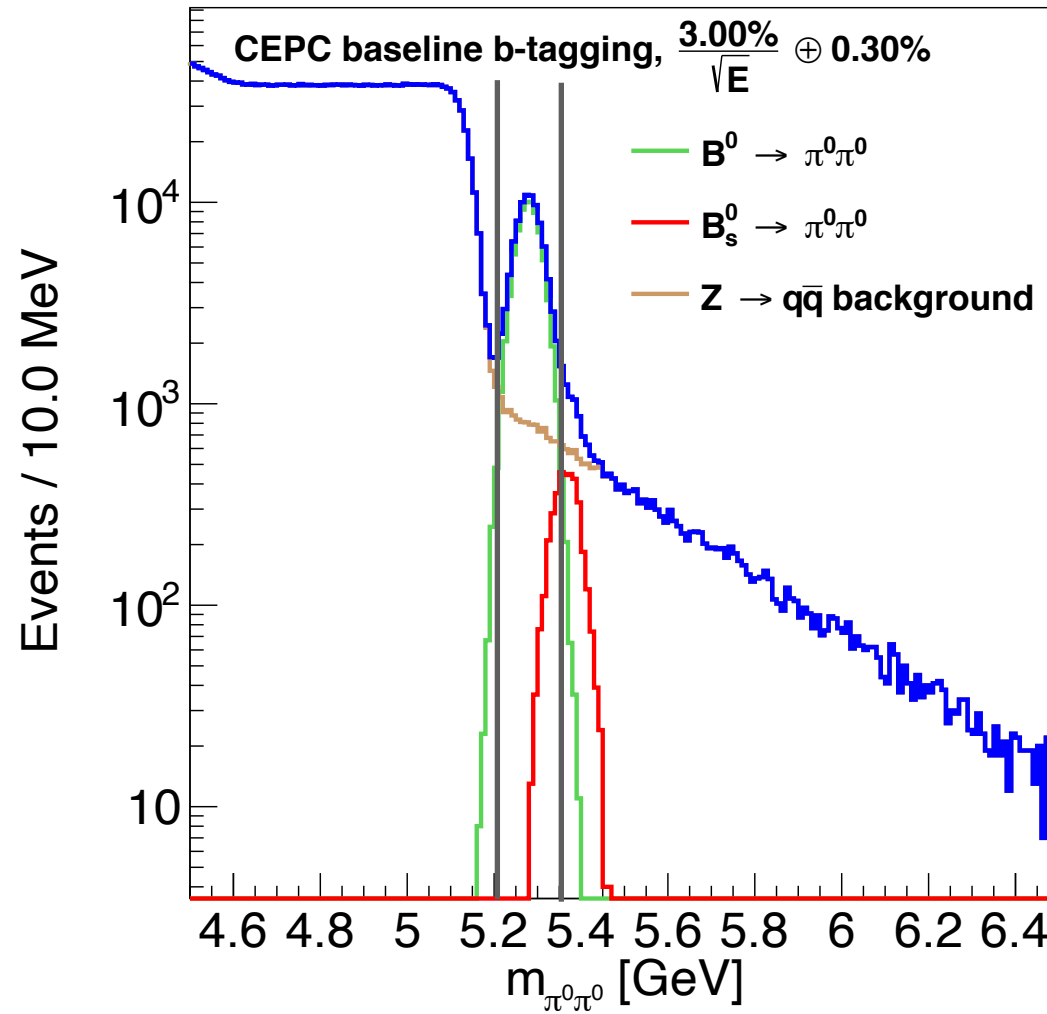
(a) Energy spectrum of π^0 pairs in $B^0 \rightarrow \pi^0\pi^0$ (left), $B_s^0 \rightarrow \pi^0\pi^0$ (middle), and $Z \rightarrow q\bar{q}$ (right) events.



(b) $\theta_{\pi^0\pi^0}$ vs $E_{\pi^0\pi^0}$ in $B^0 \rightarrow \pi^0\pi^0$ (left), $B_s^0 \rightarrow \pi^0\pi^0$ (middle), and $Z \rightarrow q\bar{q}$ (right) events.

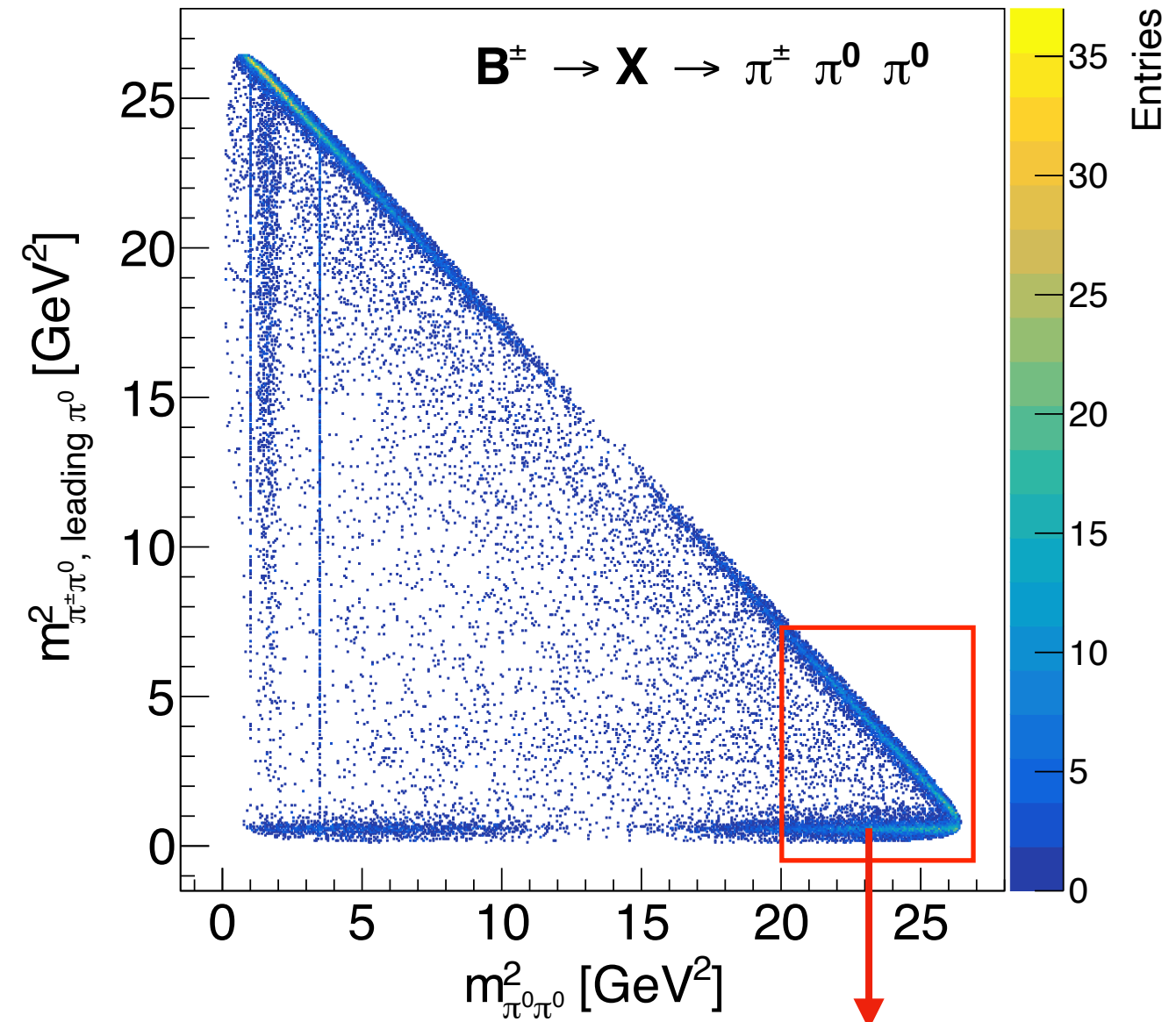
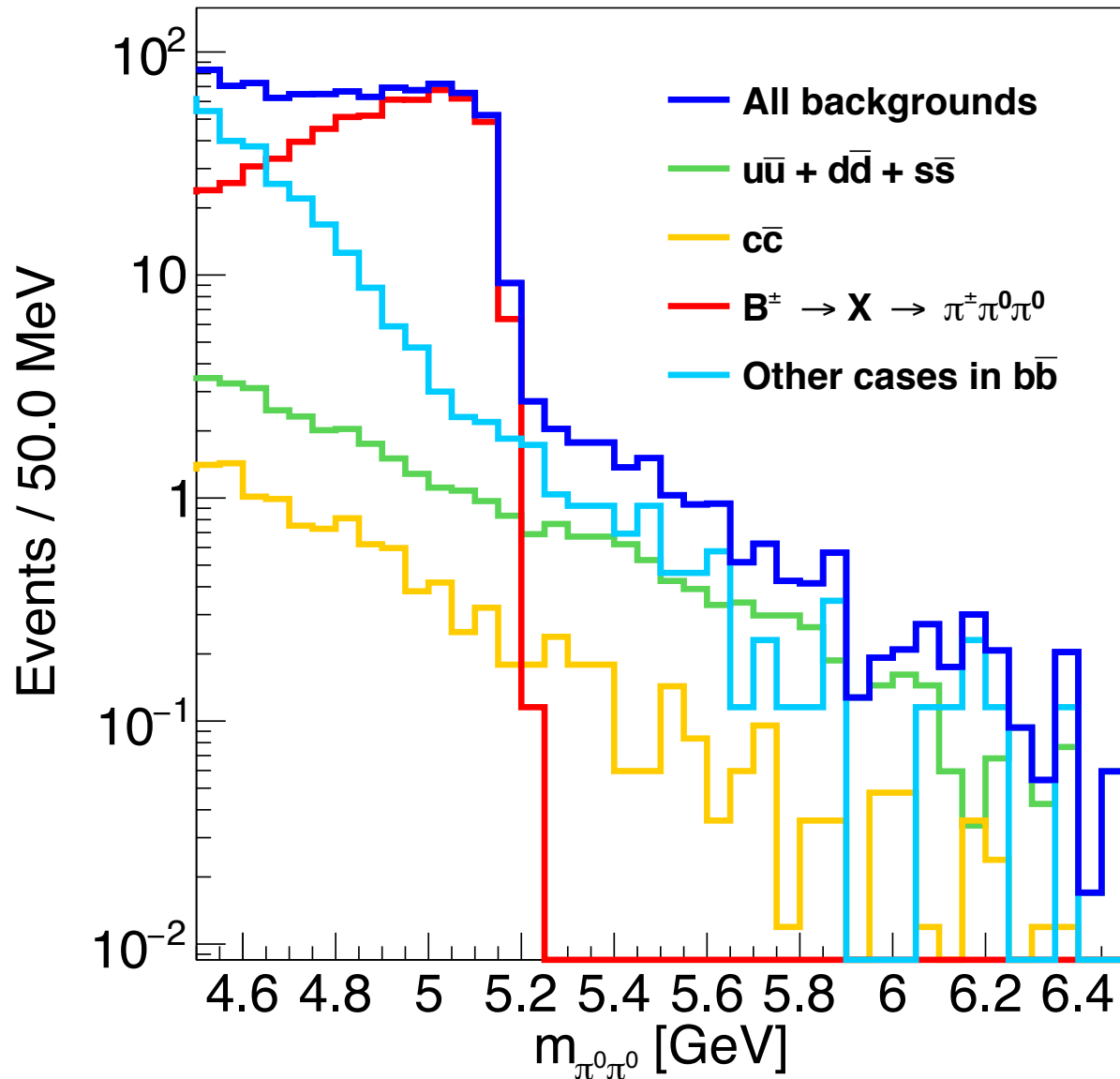
Cut chain	$B^0 \rightarrow \pi^0\pi^0$	$B_s^0 \rightarrow \pi^0\pi^0$	$q\bar{q}$	$u\bar{u}+d\bar{d}+s\bar{s}$	$c\bar{c}$	$b\bar{b}$	$\sqrt{S} + B/S$
Total generated	191113	8948	7e11 (100.00%)	4.285e11 (61.21%)	1.203e11 (17.19%)	1.512e11 (21.60%)	
b-tagging ($\epsilon_{b,c,uds \rightarrow b} = 80\%, 8.26\%, 0.85\%$)	152890	7158	1.34539e11 (100.00%)	3.64225e9 (2.70%)	9.93678e9 (7.38%)	1.2096e11 (89.92%)	
$\pi^0 \rightarrow \gamma\gamma$	147932	6959	134272699126	3605151069	9908563142	120758984915	
Lower $E_{\pi^0} > 6$ GeV	92172	4396	15490570779	843830534	1598643569	13048096676	
Higher $E_{\pi^0} > 14$ GeV	87057	4148	2534286670	307734259	314762436	1911789975	
$E_{\pi^0\pi^0} > 22$ GeV	86807	4133	2233308564	289771547	281656846	1661880170	
$\theta_{\pi^0\pi^0} < 23^\circ$	77626	3644	825367542	119076559	102055313	604235671	
$m_{\pi^0\pi^0} \in (5.2188, 5.3405)$ GeV ($2.0 \sigma_{m_{B^0}} = 2.0 \times 0.0304$ GeV)	75374	717	17896	5640	1656	10600	0.4067% $\pm 0.0106\%$
$m_{\pi^0\pi^0} \in (5.3421, 5.3917)$ GeV ($0.8 \sigma_{m_{B_s^0}} = 0.8 \times 0.0310$ GeV)	3769	2394	5477	2400	507	2570	4.5070% $\pm 0.5563\%$

Event Selection



Cut chain	$B^0 \rightarrow \pi^0 \pi^0$	$B_s^0 \rightarrow \pi^0 \pi^0$	$q\bar{q}$	$u\bar{u}+d\bar{d}+s\bar{s}$	$c\bar{c}$	$b\bar{b}$	$\sqrt{S} + B/S$
Total generated	191113	8948	7e11 (100.00%)	4.285e11 (61.21%)	1.203e11 (17.19%)	1.512e11 (21.60%)	
b-tagging ($\epsilon_{b,c,uds \rightarrow b} = 80\%, 8.26\%, 0.85\%$)	152890	7158	1.34539e11 (100.00%)	3.64225e9 (2.70%)	9.93678e9 (7.38%)	1.2096e11 (89.92%)	
$\pi^0 \rightarrow \gamma\gamma$	147932	6959	134272699126	3605151069	9908563142	120758984915	
Lower $E_{\pi^0} > 6$ GeV	92172	4396	15490570779	843830534	1598643569	13048096676	
Higher $E_{\pi^0} > 14$ GeV	87057	4148	2534286670	307734259	314762436	1911789975	
$E_{\pi^0 \pi^0} > 22$ GeV	86807	4133	2233308564	289771547	281656846	1661880170	
$\theta_{\pi^0 \pi^0} < 23^\circ$	77626	3644	825367542	119076559	102055313	604235671	
Optimized mass window							
$m_{\pi^0 \pi^0} \in (5.2188, 5.3405) \text{ GeV}$ ($2.0 \sigma_{m_{B^0}} = 2.0 \times 0.0304 \text{ GeV}$)	75374	717	17896	5640	1656	10600	0.4067% $\pm 0.0106\%$
$m_{\pi^0 \pi^0} \in (5.3421, 5.3917) \text{ GeV}$ ($0.8 \sigma_{m_{B_s^0}} = 0.8 \times 0.0310 \text{ GeV}$)	3769	2394	5477	2400	507	2570	4.5070% $\pm 0.5563\%$

Background components



$\sim 93\% B^\pm \rightarrow \rho(770)^\pm \pi^0, \rho(770)^\pm \rightarrow \pi^\pm \pi^0$
 $\sim 7\% B^\pm \rightarrow \pi^\pm \pi^0 \pi^0$

Kinematic constraint of $B \rightarrow X \rightarrow \pi^\pm \pi^0 \pi^0 \rightarrow$ cut-off ~ 5.2 GeV on $m_{\pi^0\pi^0}$.

Dependence on b-tagging performance

Three b-tagging conditions, at $3\%/\sqrt{E_T} + 0.3\%$

Accuracy

$B^0 \rightarrow \pi^0 \pi^0$

b-tagging	Mass window (GeV)	$n \sigma_{m_B}$	$B^0 \rightarrow \pi^0 \pi^0$	$B_s^0 \rightarrow \pi^0 \pi^0$	$q\bar{q}$	$u\bar{u} + d\bar{d} + s\bar{s}$	$c\bar{c}$	$b\bar{b}$	$\sqrt{S + B}/S$
No b-tagging ($\epsilon_{b,c,uds \rightarrow b} = 100\%, 100\%, 100\%$)	(5.2370, 5.3222)	1.4	85986	311	517718	494139	15549	8030	$0.9038\% \pm 0.0308\%$
CEPC baseline b-tagging ($\epsilon_{b,c,uds \rightarrow b} = 80\%, 8.26\%, 0.85\%$)	(5.2188, 5.3405)	2.0	75374	717	17896	5640	1656	10600	$0.4067\% \pm 0.0106\%$
Ideal b-tagging ($\epsilon_{b,c,uds \rightarrow b} = 100\%, 0\%, 0\%$)	(5.2188, 5.3405)	2.0	94217	896	13250	0	0	13250	$0.3494\% \pm 0.0047\%$

$B_s \rightarrow \pi^0 \pi^0$

b-tagging	Mass window (GeV)	$n \sigma_{m_B}$	$B^0 \rightarrow \pi^0 \pi^0$	$B_s^0 \rightarrow \pi^0 \pi^0$	$q\bar{q}$	$u\bar{u} + d\bar{d} + s\bar{s}$	$c\bar{c}$	$b\bar{b}$	$\sqrt{S + B}/S$
No b-tagging ($\epsilon_{b,c,uds \rightarrow b} = 100\%, 100\%, 100\%$)	(5.3328, 5.4010)	1.1	8563	3613	353469	338838	9411	5220	$16.7354\% \pm 0.7580\%$
CEPC baseline b-tagging ($\epsilon_{b,c,uds \rightarrow b} = 80\%, 8.26\%, 0.85\%$)	(5.3421, 5.3917)	0.8	3769	2394	5477	2400	507	2570	$4.5070\% \pm 0.5563\%$
Ideal b-tagging ($\epsilon_{b,c,uds \rightarrow b} = 100\%, 0\%, 0\%$)	(5.3421, 5.3917)	0.8	4712	2992	3212	0	0	3212	$3.4917\% \pm 0.1953\%$

2~3 times

~1.2 times

No b-tagging



CEPC baseline b-tagging

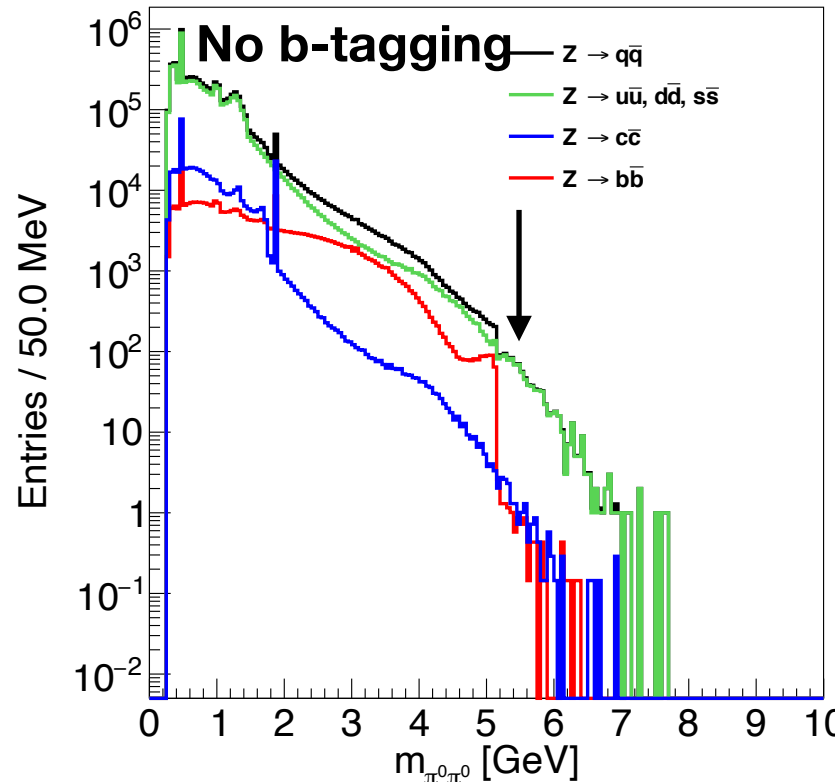


comparable

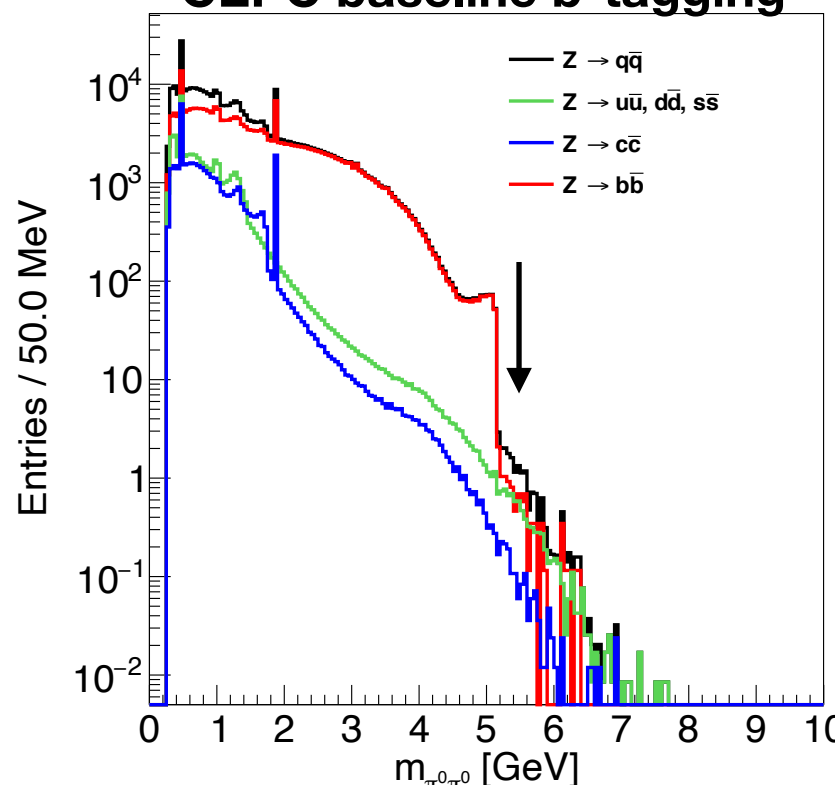
Ideal b-tagging

Dependence on b-tagging performance

b-tagging is essential to reduce the hard combinatorial background in non- bb events



CEPC baseline b-tagging



π^0 s in light-quark events (mainly from hadronization) are harder than those in cc and bb events (mainly from c and b hadrons)

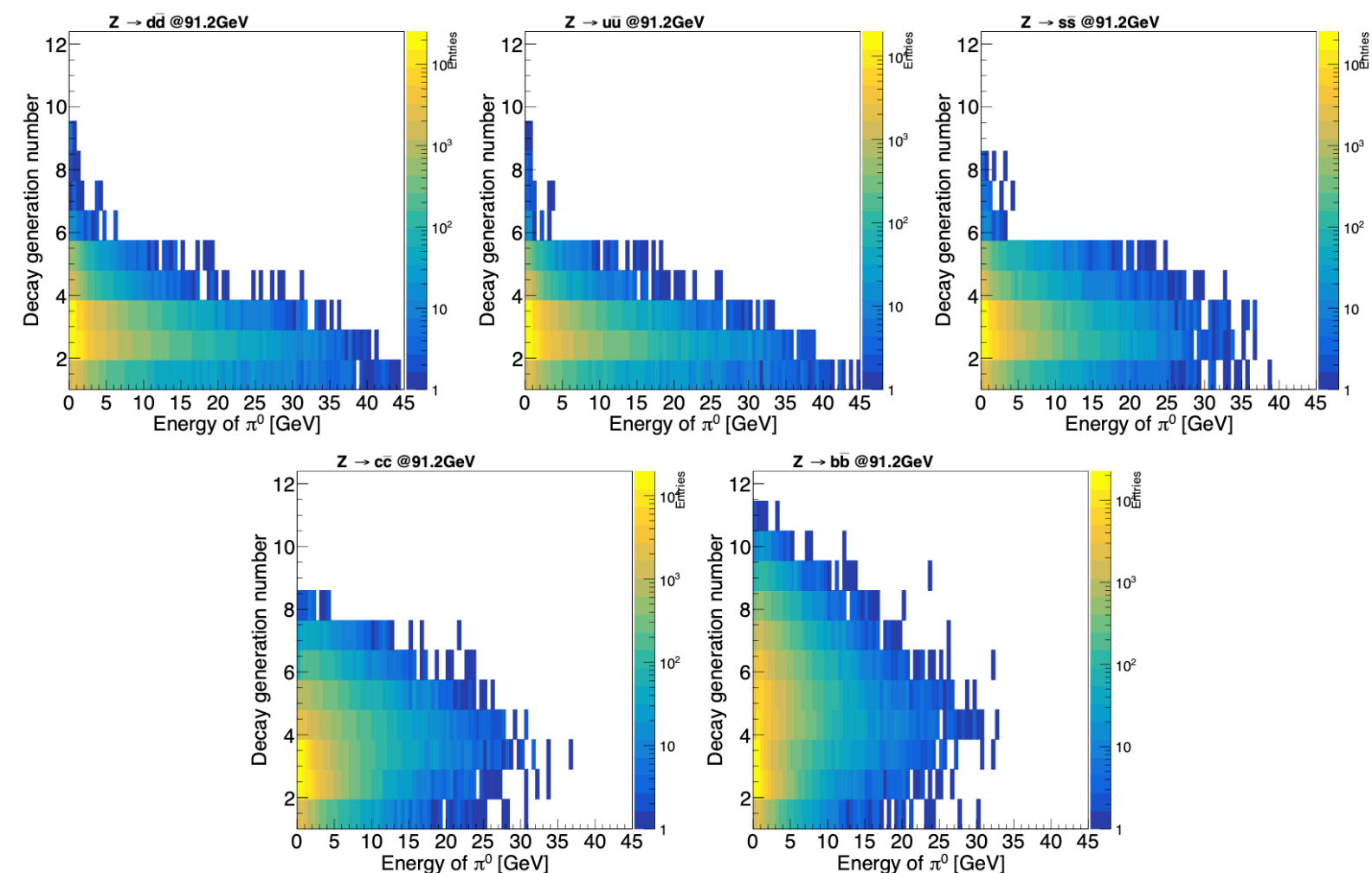
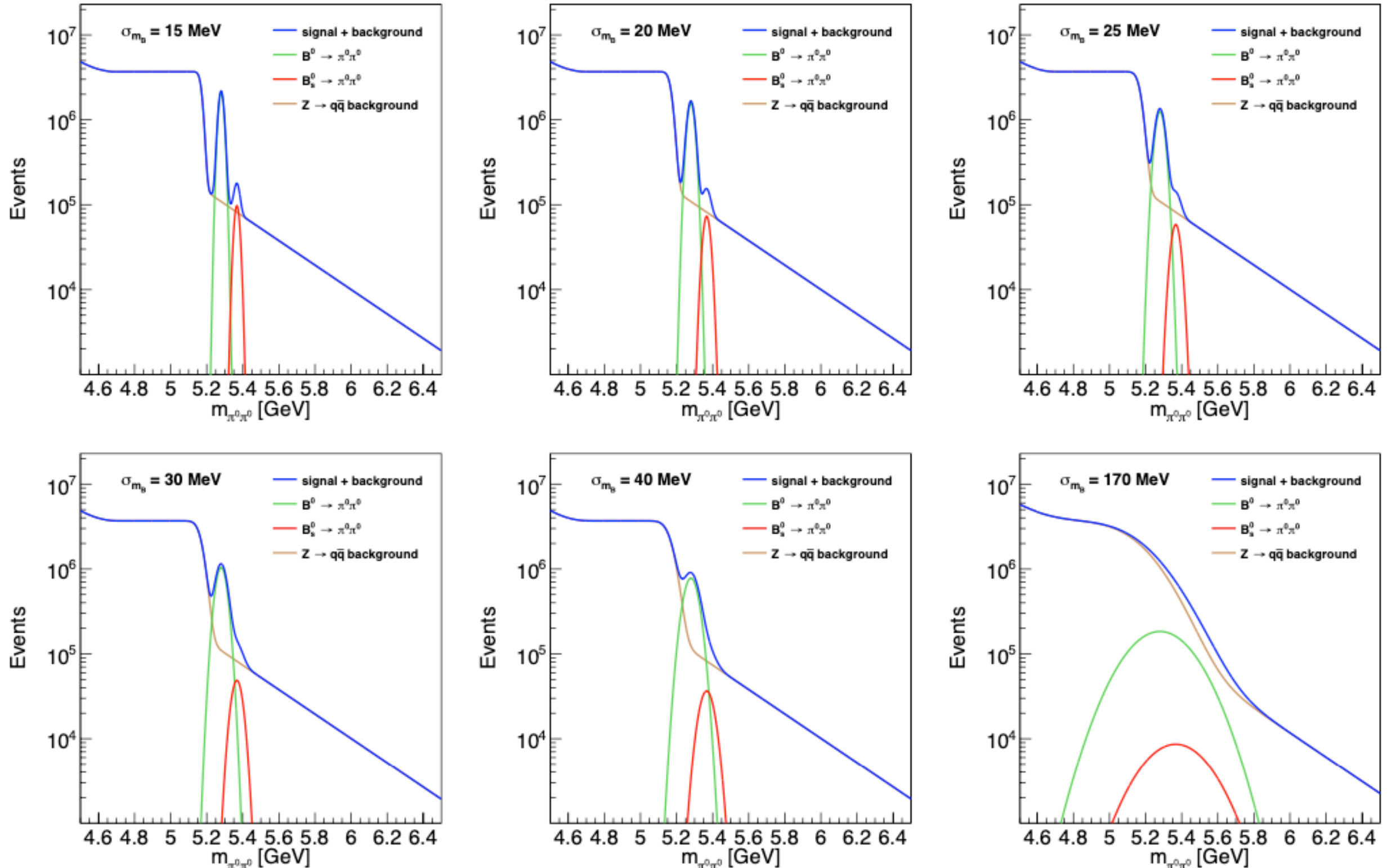


Figure 5: Decay generation number of π^0 vs E_{π^0} in $Z \rightarrow u\bar{u}$, $Z \rightarrow d\bar{d}$, $Z \rightarrow s\bar{s}$, $Z \rightarrow c\bar{c}$, $Z \rightarrow b\bar{b}$ events.

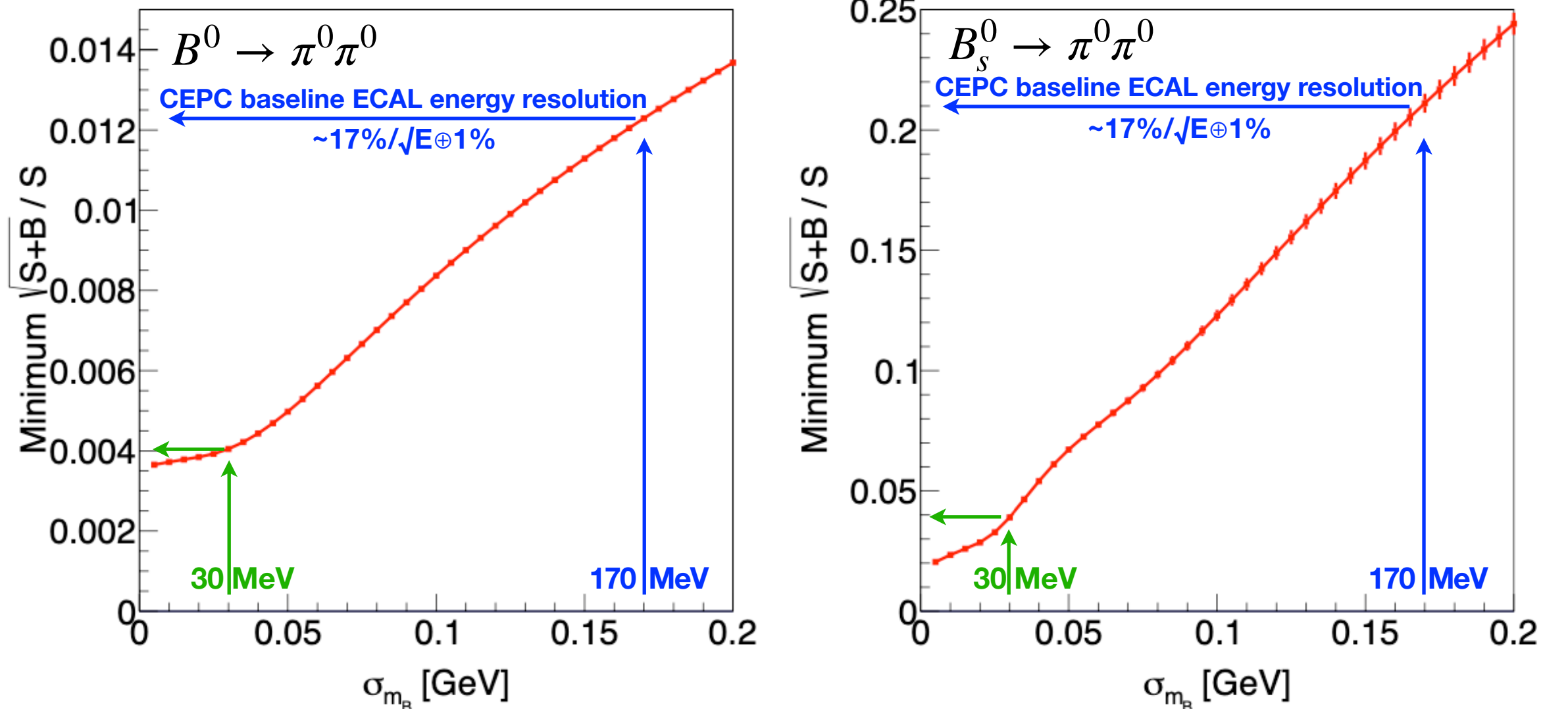
Dependence on B mass resolution

with CEPC baseline b-tagging



Dependence on B mass resolution

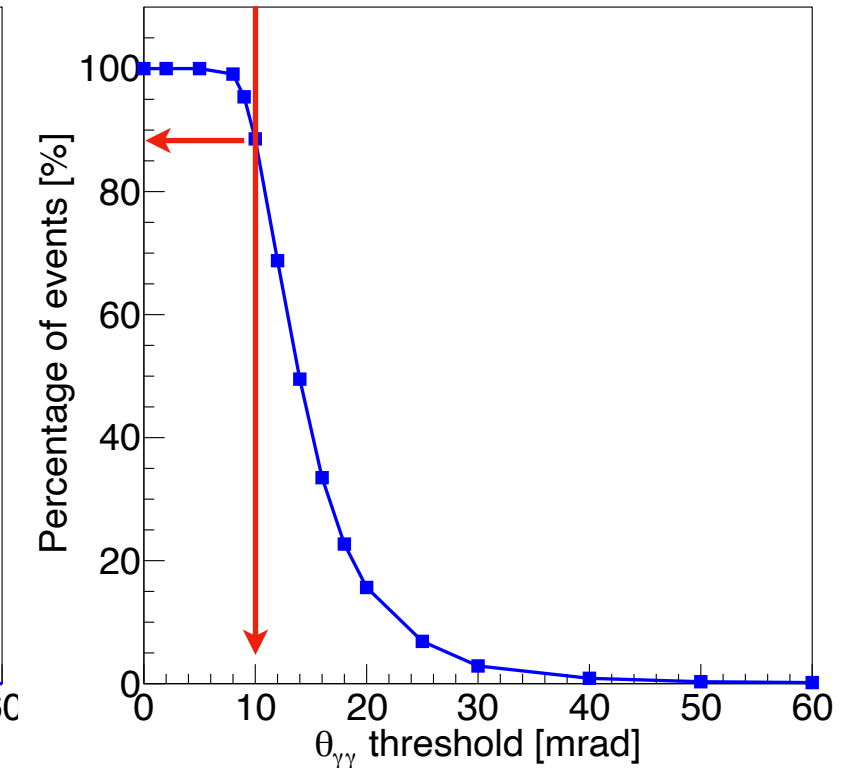
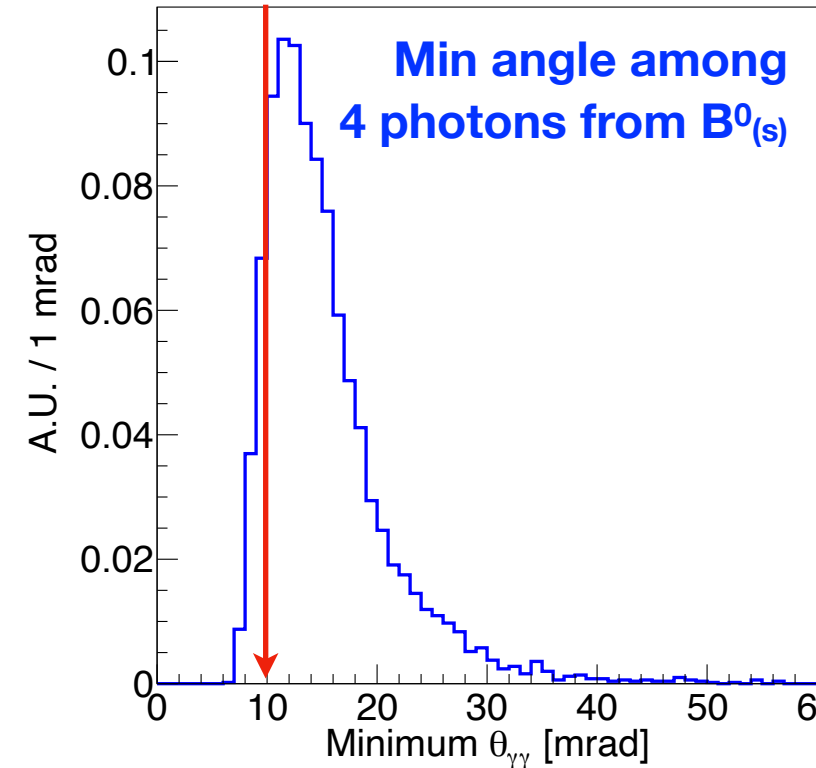
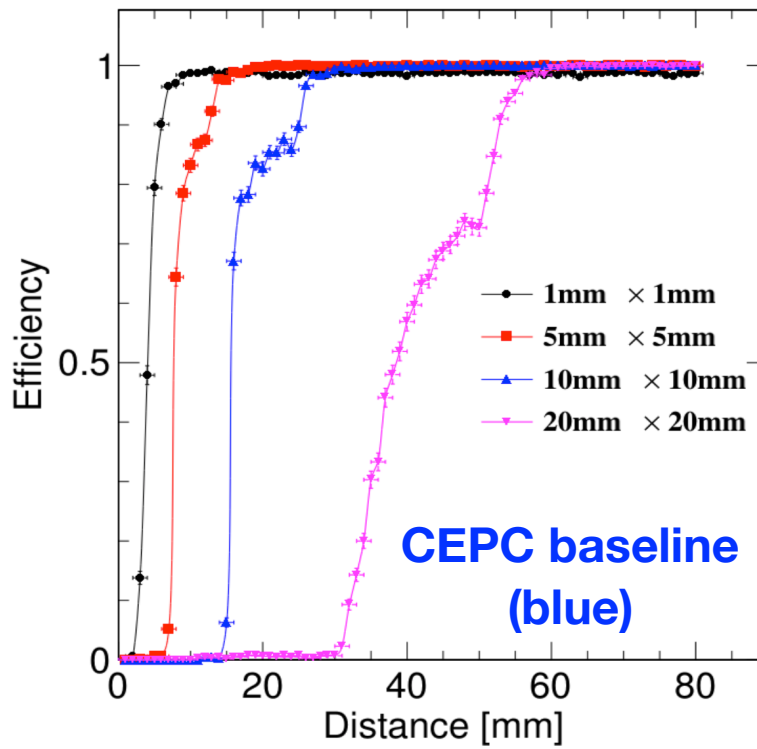
with CEPC baseline b-tagging



Accuracy	$B^0 \rightarrow \pi^0 \pi^0$	$B_s^0 \rightarrow \pi^0 \pi^0$	
$17\%/\sqrt{E} + 1\% \text{ (CEPC baseline)}$	$\sim 1.2\%$	$\sim 21\%$	
$3\%/\sqrt{E} + 0.3\% \text{ (\sigma_{m_B} \sim 30\text{ MeV})}$	$\sim 0.4\%$	$\sim 4\%$	3~5 times improvement

Estimation of other Effects

- Photon conversion
 - Central region: **5–10%** || Forward region: **~25%**
 - **~80%** can be recovered
 - Average conversion rate: **3% (each photon)**
→ **~11.5% efficiency lost of $B^0_{(s)} \rightarrow \pi^0\pi^0$ reconstruction**
- Photon separation (especially di-photon merging)
 - **2 cm** → **80% separation efficiency (5 GeV, CEPC baseline)**
 - **2 cm** → **10 mrad angular separation (ECAL $R_{inner} = 2m$)**
→ **~10% efficiency lost of $B^0_{(s)} \rightarrow \pi^0\pi^0$ reconstruction**



👉 **Estimation: ~20% efficiency lost → 10% accuracy degradation**

Estimation of other Effects

More realistic results when using CEPC baseline b-tagging

Accuracy	$B^0 \rightarrow \pi^0\pi^0$	$B_s^0 \rightarrow \pi^0\pi^0$
17%/\sqrt{E} ± 1% (CEPC baseline)	~1.32%	~23.1%
3%/\sqrt{E} ± 0.3% ($\sigma_{mB} \sim 30$ MeV)	~0.44%	~4.4%

↓

~36 times better than the current world average precision

~5 times better than the anticipated accuracy at the Belle II

Measurement of $B^0 \rightarrow \pi^0\pi^0$

Current world average precision

~16%

Anticipated Accuracy at Belle II

~2.3%

E. Kou et al.

$\Gamma(B^0 \rightarrow \pi^0\pi^0)/\Gamma_{\text{total}}$				
VALUE (10^{-6})	CL%	DOCUMENT ID	TECN	COMMENT
1.59 ± 0.26	OUR AVERAGE	Error includes scale factor of 1.4.		
1.31 ± 0.19 ± 0.19	¹ JULIUS	2017	BELL	$e^+ e^- \rightarrow \Upsilon(4S)$
1.83 ± 0.21 ± 0.13	¹ LEES	2013D	BABR	$e^+ e^- \rightarrow \Upsilon(4S)$

Table 90. Statistical uncertainties $\Delta A_{\pi^0\pi^0}$, $\Delta S_{\pi^0\pi^0}$, and $\Delta \mathcal{B}_{\pi^0\pi^0}/\mathcal{B}_{\pi^0\pi^0}$ for different input values of $A_{\pi^0\pi^0}$ and $S_{\pi^0\pi^0}$ used for the generation of signal MC.

Input values	Time-dependent		Time-integrated		
	$A_{\pi^0\pi^0}$	$S_{\pi^0\pi^0}$	$\Delta A_{\pi^0\pi^0}$	$\Delta S_{\pi^0\pi^0}$	$\Delta \mathcal{B}_{\pi^0\pi^0}/\mathcal{B}_{\pi^0\pi^0}$ [%]
0.34 [650]	0.65 [650]	0.22	0.28	0.03	2.2
0.43 [88]	0.79	0.23	0.29	0.03	2.2
0.14 [712]	0.83	0.21	0.26	0.03	2.4
0.14 [712]	0.40	0.20	0.29	0.03	2.3
0.14 [712]	-0.61	0.22	0.27	0.03	2.3
0.14 [712]	-0.94	0.22	0.28	0.03	2.4

value $S_{\pi^0\pi^0} = 0.65$ [650]. The assumed branching fraction $\mathcal{B}_{\pi^0\pi^0} = 1.91 \cdot 10^{-6}$ [88] yields 15 068 signal events for the time-integrated analysis and 271 for the time-dependent analysis. The latter number of events is composed of 147 signal events with Dalitz decays and 124 signal events with conversions. These two types of signal events are considered as two independent signal components

Summary

$B^0_{(s)} \rightarrow \pi^0\pi^0$ are important to understand

- $B^0 \rightarrow \pi^0\pi^0$: CKM angle α and $B \rightarrow \pi\pi$ puzzle
- $B^0_s \rightarrow \pi^0\pi^0$: annihilation mechanism

Fast Simulation is used to study the dependence of $B^0_{(s)} \rightarrow \pi^0\pi^0$ accuracy on

❖ b-tagging:

- is essential to reduce the hard combinatorial background in non- $b\bar{b}$ events
- CEPC baseline b-tagging can improve the measurement accuracy by 2-3 times compared with the case with no b-tagging

❖ B mass resolution (σ_{mB}):

- 2σ separation of B^0 and B_s requires σ_{mB} better than 30 MeV ($\sim 3\%/\sqrt{E} \oplus 0.3\%$).

Accuracy with CEPC baseline b-tagging	$B^0 \rightarrow \pi^0\pi^0$	$B^0_s \rightarrow \pi^0\pi^0$	
17%/ $\sqrt{E} \oplus 1\%$ (CEPC baseline)	~1.32%	~23.1%	
3%/ $\sqrt{E} \oplus 0.3\%$ ($\sigma_{mB} \sim 30$ MeV)	~0.44%	~4.4%	3~5 times improvement

~36 times better than the current world average precision

~5 times better than the anticipated accuracy at the Belle II

→ enable the more precise determination of the CKM angle α (Φ_2)

Backup

CKM Quark-Mixing Matrix

12.3 Phases of CKM elements

As can be seen from Fig. 12.1, the angles of the unitarity triangle are

$$\begin{aligned}\beta &= \phi_1 = \arg \left(-\frac{V_{cd} V_{cb}^*}{V_{td} V_{tb}^*} \right), \\ \alpha &= \phi_2 = \arg \left(-\frac{V_{td} V_{tb}^*}{V_{ud} V_{ub}^*} \right), \\ \gamma &= \phi_3 = \arg \left(-\frac{V_{ud} V_{ub}^*}{V_{cd} V_{cb}^*} \right).\end{aligned}\quad (12.16)$$

Since CP violation involves phases of CKM elements, many measurements of CP -violating observables can be used to constrain these angles and the $\bar{\rho}, \bar{\eta}$ parameters.

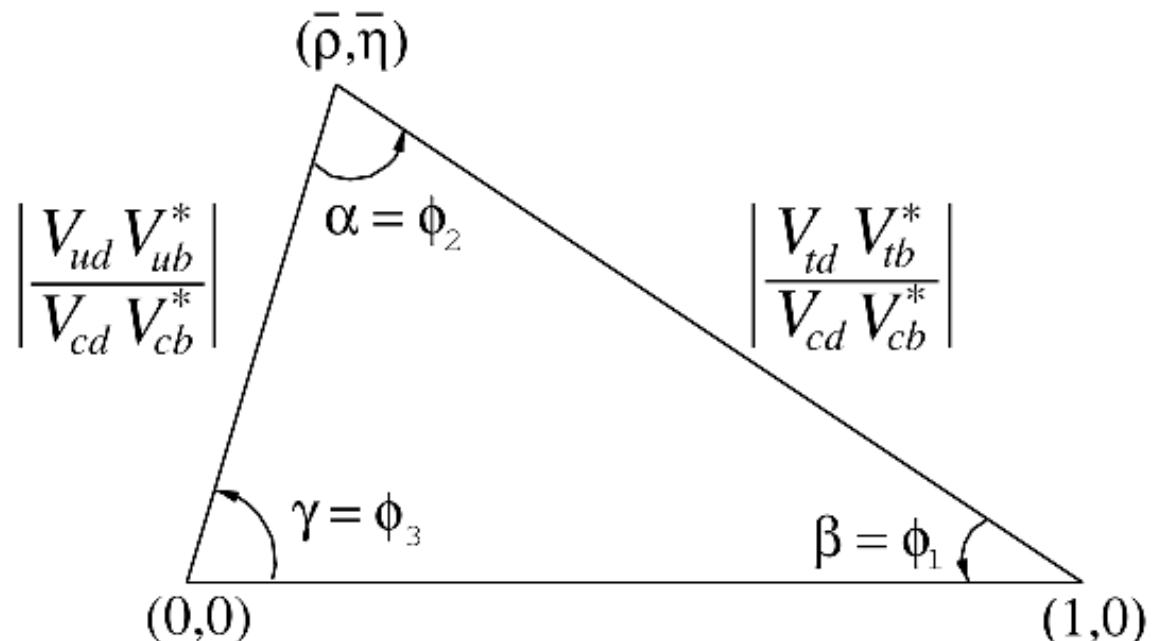


Figure 12.1: Sketch of the unitarity triangle.

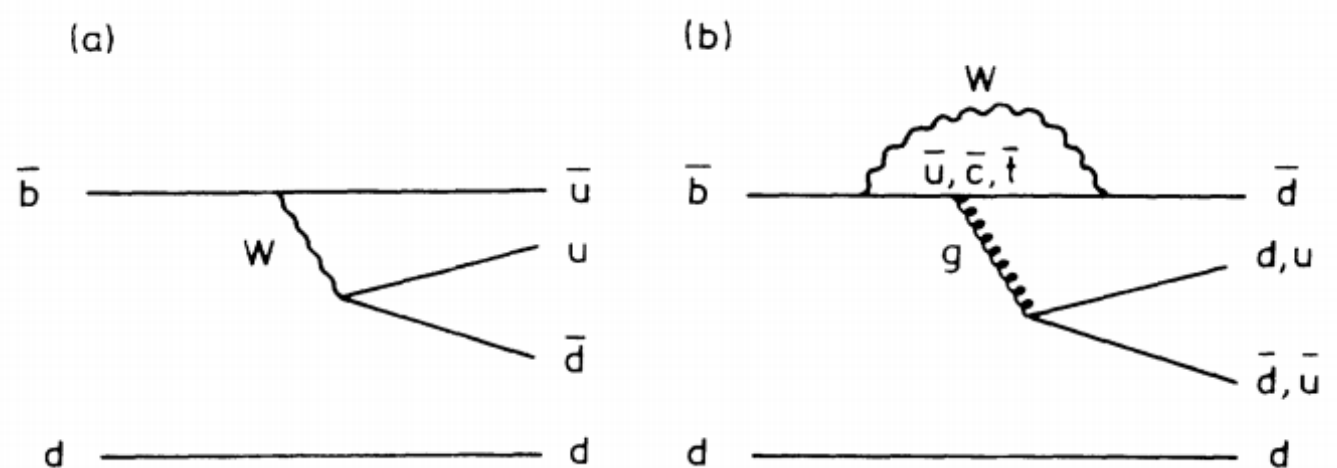
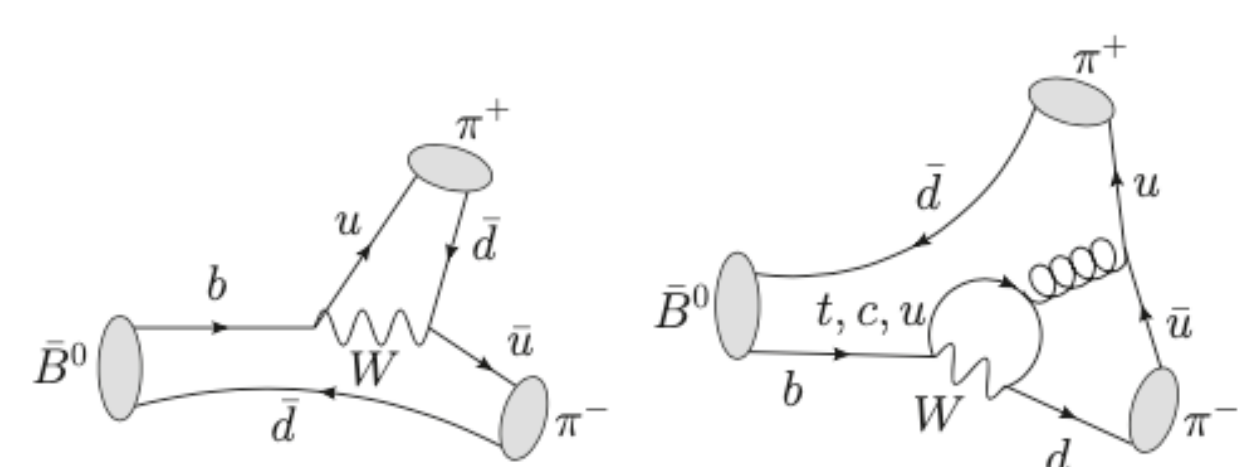


FIG. 1. (a) Tree-level and (b) penguin diagrams for the decay $B_d^0 \rightarrow \pi\pi$.

b-hadron yield

Hadrons	Belle II	LHCb (300 fb ⁻¹)	CEPC (10 ¹² Z)
B^0, \bar{B}^0	5.3×10^{10}	$\sim 6 \times 10^{13}$	1.2×10^{11}
B^\pm	5.6×10^{10}	$\sim 6 \times 10^{13}$	1.2×10^{11}
B_s, \bar{B}_s	5.7×10^8	$\sim 2 \times 10^{13}$	3.2×10^{10}
B_c^\pm	-	$\sim 4 \times 10^{11}$	2.2×10^8
$\Lambda_b, \bar{\Lambda}_b$	-	$\sim 2 \times 10^{13}$	1.0×10^{10}

TABLE II. The number of b -hadrons expected to be produced in Belle II, LHCb and CEPC. Here, the Belle II column corresponds to its $50 \text{ ab}^{-1} \Upsilon(4S)$ run and its $5 \text{ ab}^{-1} \Upsilon(5S)$ run.

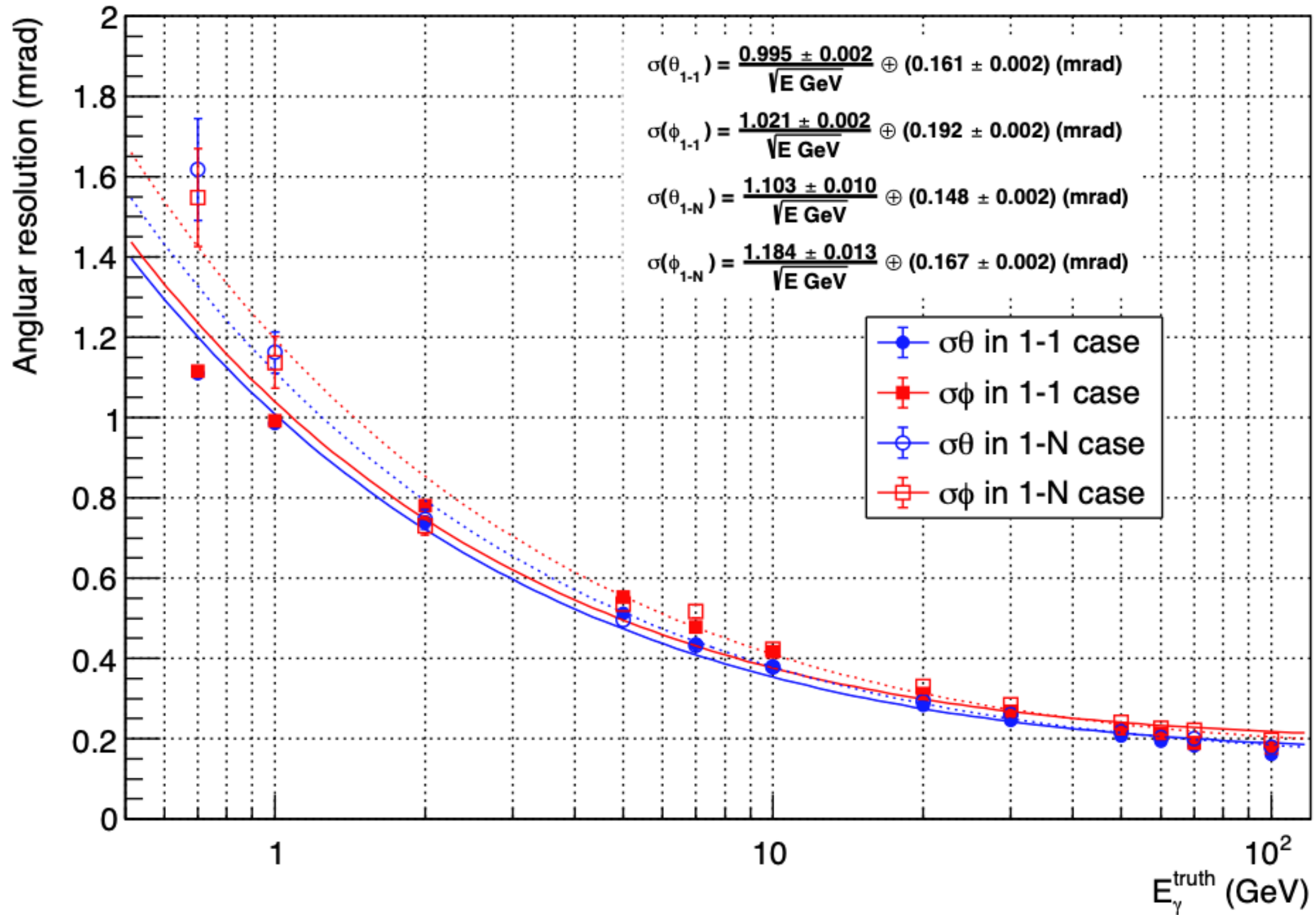
Belle II Physics Book

For this study, we generate and reconstruct signal MC events with $B_{\text{sig}} \rightarrow \pi^0 \pi^0$ and $B_{\text{tag}} \rightarrow \text{generic}$. Assuming that $\mathcal{B}_{\pi^0 \pi^0} = 1.91 \cdot 10^{-6}$ [88], the total number of expected events in 50 ab^{-1} is about 103 000. For the CP analyses, the following three decay modes are considered as signal:

- $B_{\text{sig}}^0 \rightarrow \pi_{\gamma\gamma}^0 (\rightarrow \gamma\gamma) \pi_{\gamma\gamma}^0 (\rightarrow \gamma\gamma)$,
- $B_{\text{sig}}^0 \rightarrow \pi_{\text{dal}}^0 (\rightarrow e^+ e^- \gamma) \pi_{\gamma\gamma}^0 (\rightarrow \gamma\gamma)$,
- $B_{\text{sig}}^0 \rightarrow \pi_{\gamma c\gamma}^0 (\rightarrow \gamma_c (\rightarrow e^+ e^-) \gamma) \pi_{\gamma\gamma}^0 (\rightarrow \gamma\gamma)$.

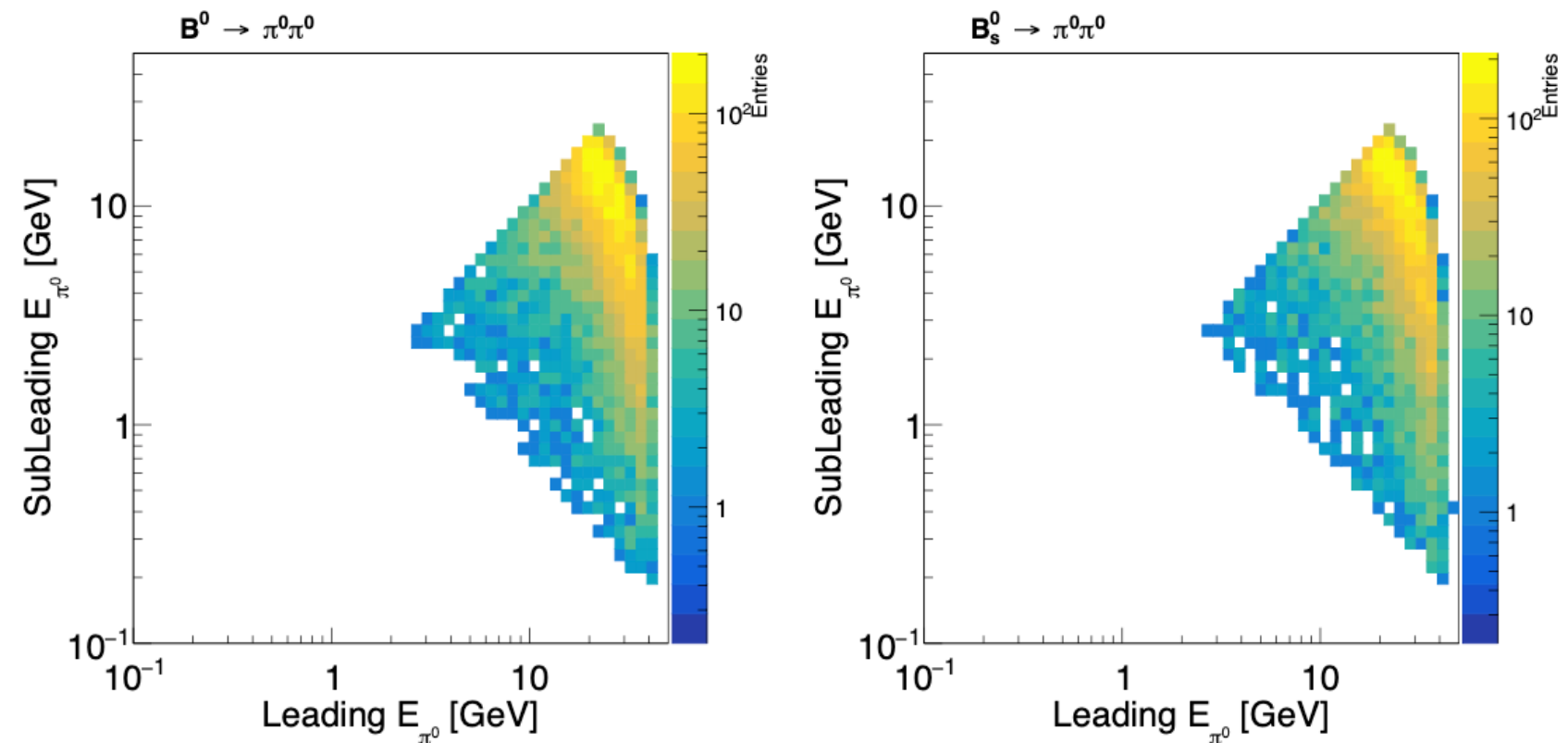
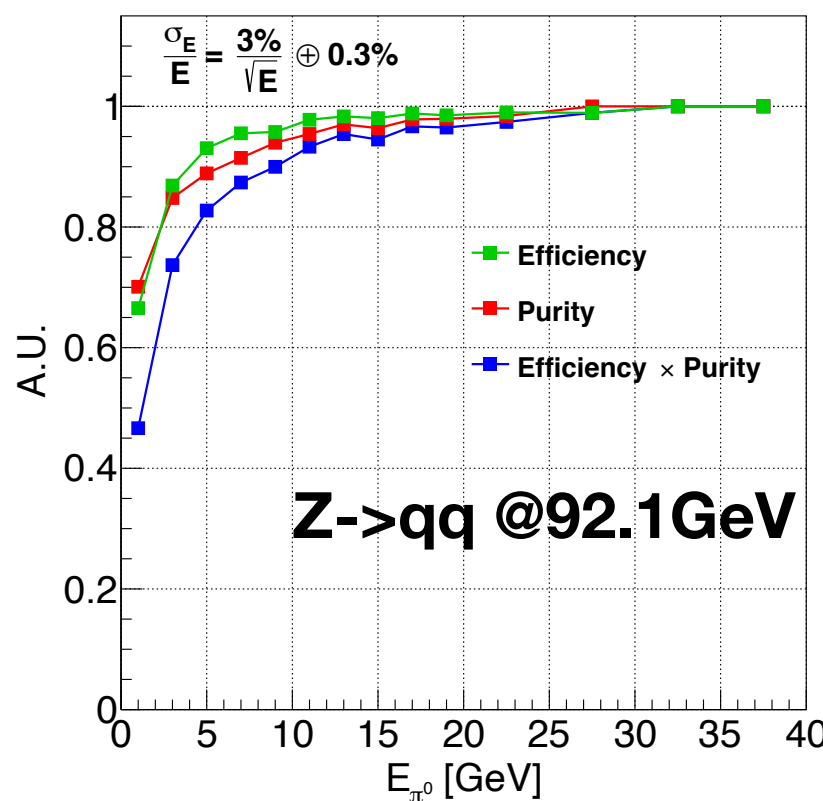
Single Photon Angular Resolution

CEPC baseline full simulation results by Yuzhi



Event Selection

Cut chain	$B^0 \rightarrow \pi^0\pi^0$	$B_s^0 \rightarrow \pi^0\pi^0$	$q\bar{q}$	$u\bar{u}+d\bar{d}+s\bar{s}$	$c\bar{c}$	$b\bar{b}$	$\sqrt{S + B/S}$
Total generated	191113	8948	7e11 (100.00%)	4.285e11 (61.21%)	1.203e11 (17.19%)	1.512e11 (21.60%)	
b-tagging ($\epsilon_{b,c,uds \rightarrow b} = 80\%, 8.26\%, 0.85\%$)	152890	7158	1.34539e11 (100.00%)	3.64225e9 (2.70%)	9.93678e9 (7.38%)	1.2096e11 (89.92%)	
$\pi^0 \rightarrow \gamma\gamma$	147932	6959	134272699126	3605151069	9908563142	120758984915	
Lower $E_{\pi^0} > 6$ GeV	92172	4396	15490570779	843830534	1598643569	13048096676	
Higher $E_{\pi^0} > 14$ GeV	87057	4148	2534286670	307734259	314762436	1911789975	
$E_{\pi^0\pi^0} > 22$ GeV	86807	4133	2233308564	289771547	281656846	1661880170	
$\theta_{\pi^0\pi^0} < 23^\circ$	77626	3644	825367542	119076559	102055313	604235671	
$m_{\pi^0\pi^0} \in (5.2188, 5.3405)$ GeV ($2.0 \sigma_{m_{B^0}} = 2.0 \times 0.0304$ GeV)	75374	717	17896	5640	1656	10600	0.4067% $\pm 0.0106\%$
$m_{\pi^0\pi^0} \in (5.3421, 5.3917)$ GeV ($0.8 \sigma_{m_{B_s^0}} = 0.8 \times 0.0310$ GeV)	3769	2394	5477	2400	507	2570	4.5070% $\pm 0.5563\%$

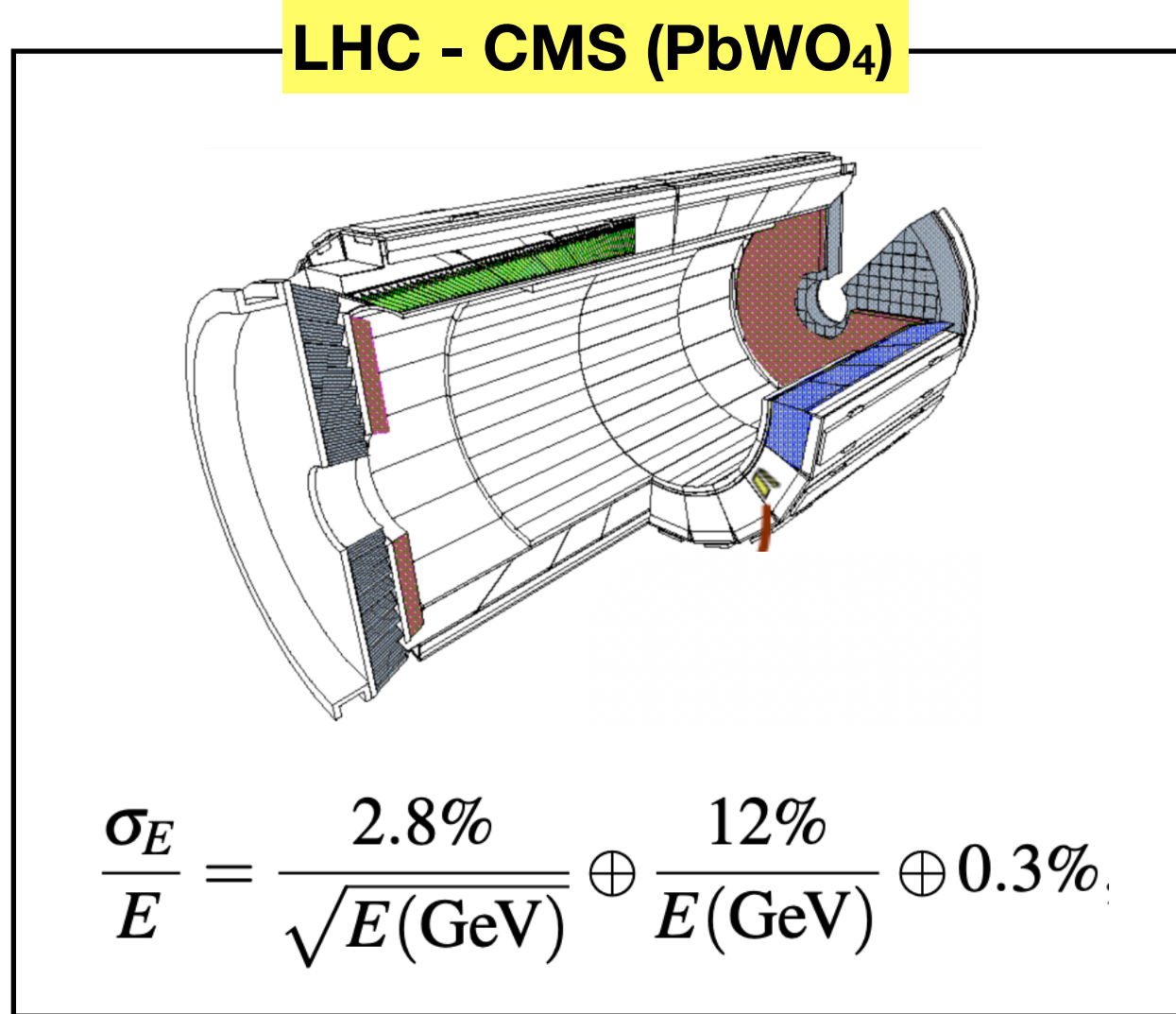


Results at a benchmark detector setup

A **benchmark** detector setup for $B^0_{(s)} \rightarrow \pi^0\pi^0$ measurement

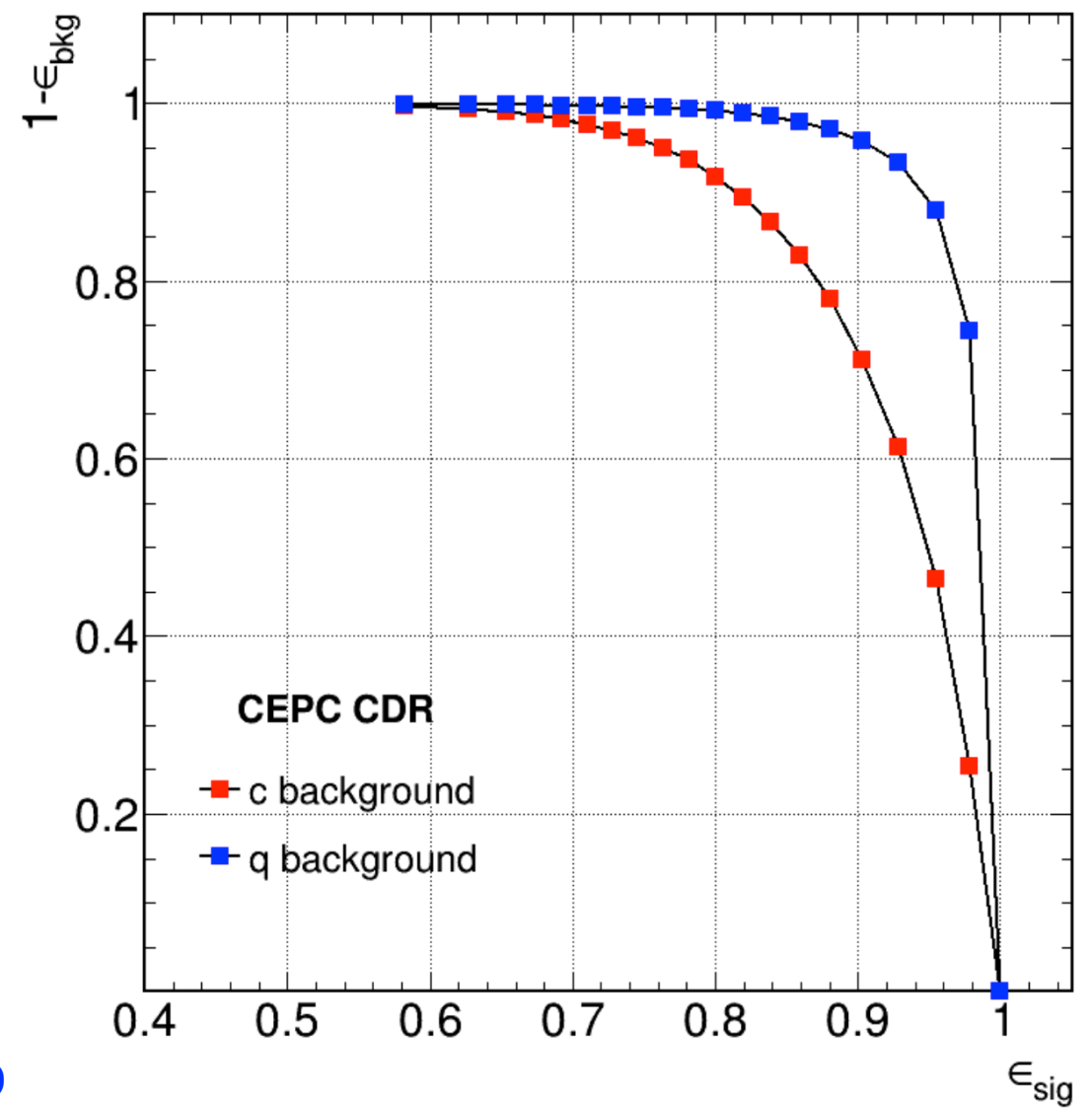
ECAL energy resolution

$$3\%/\sqrt{E} \oplus 0.3\%$$

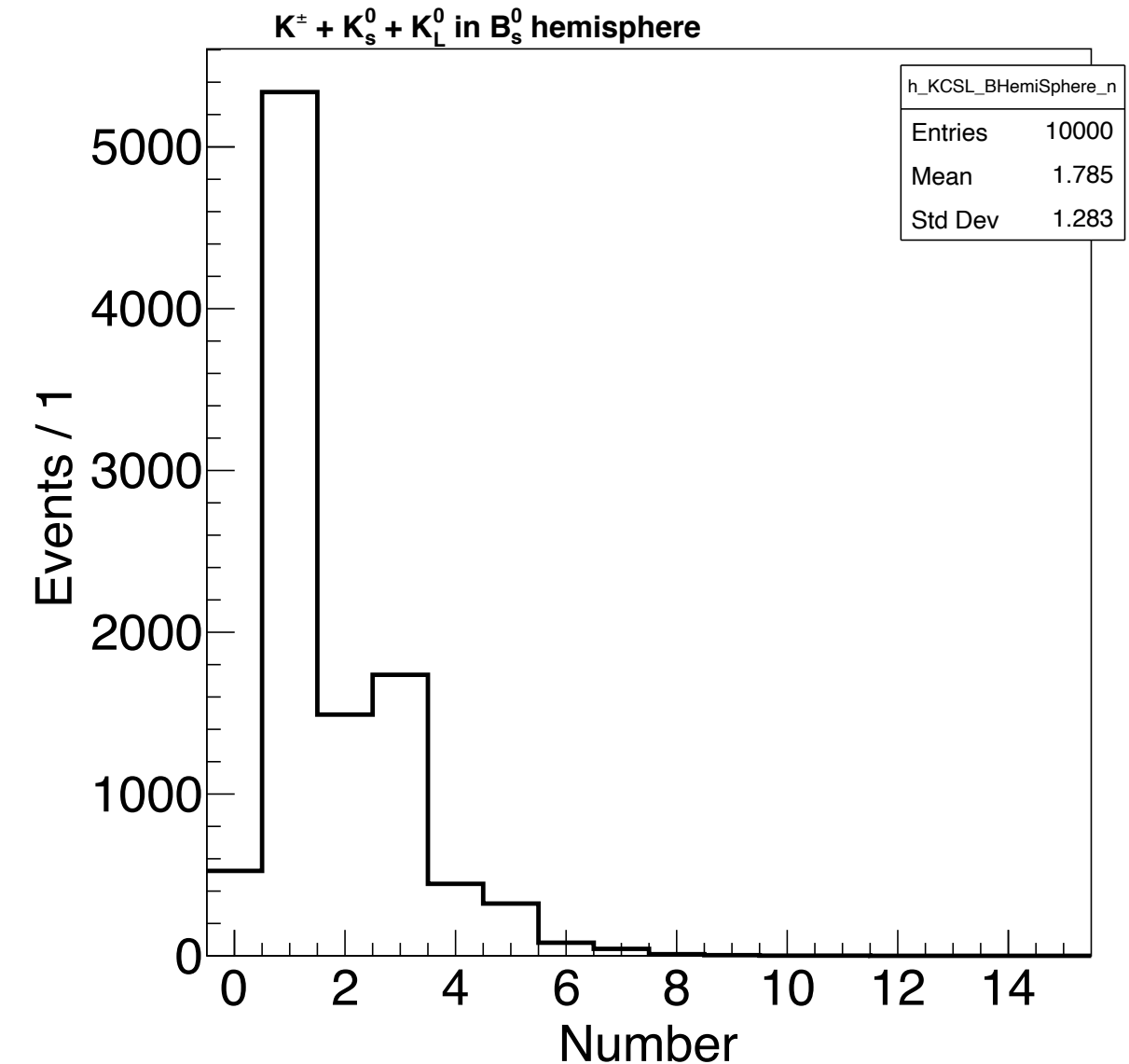
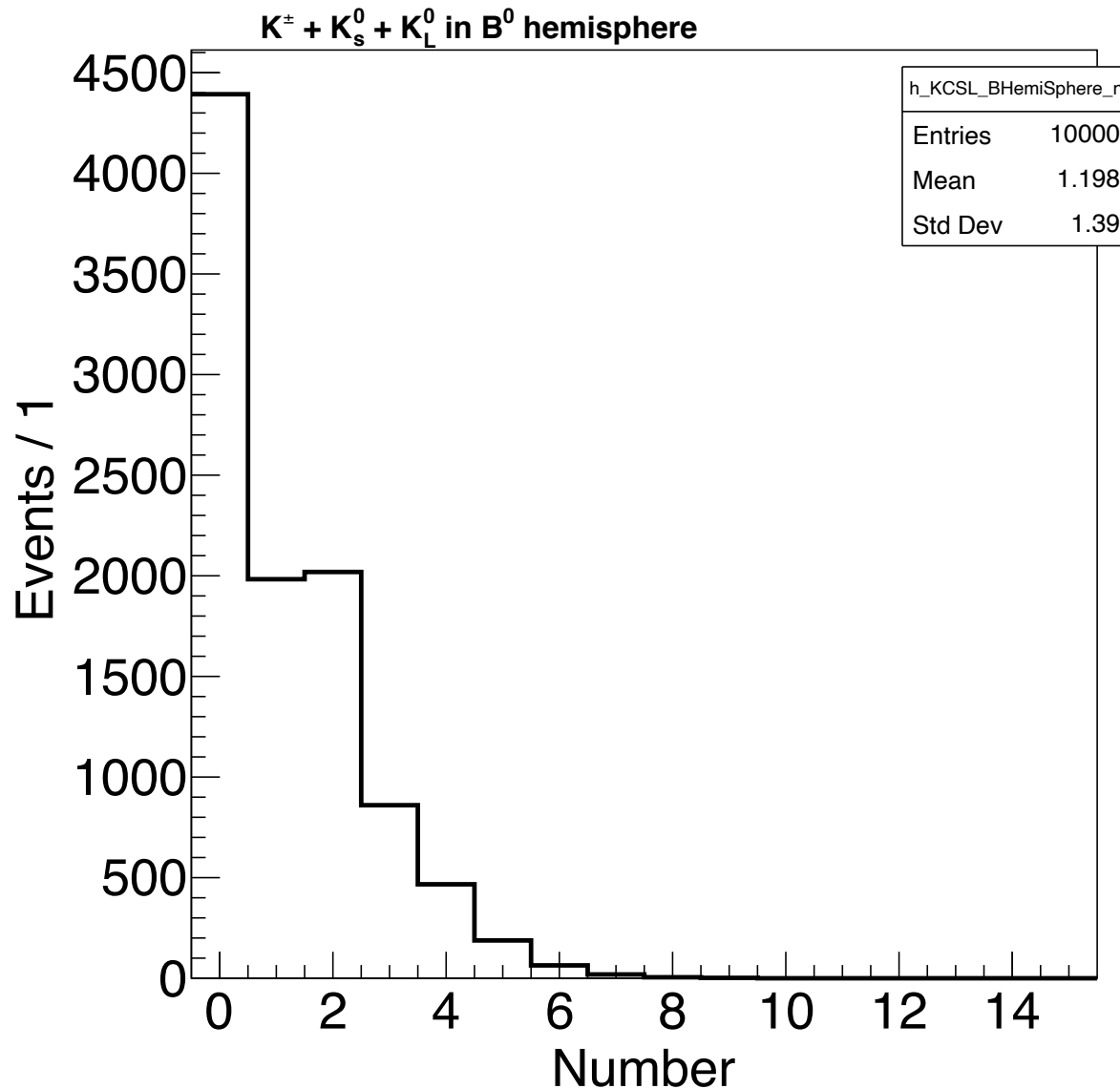


b-tagging

CEPC baseline b-tagging
80% *efficiency* and 90% *purity*



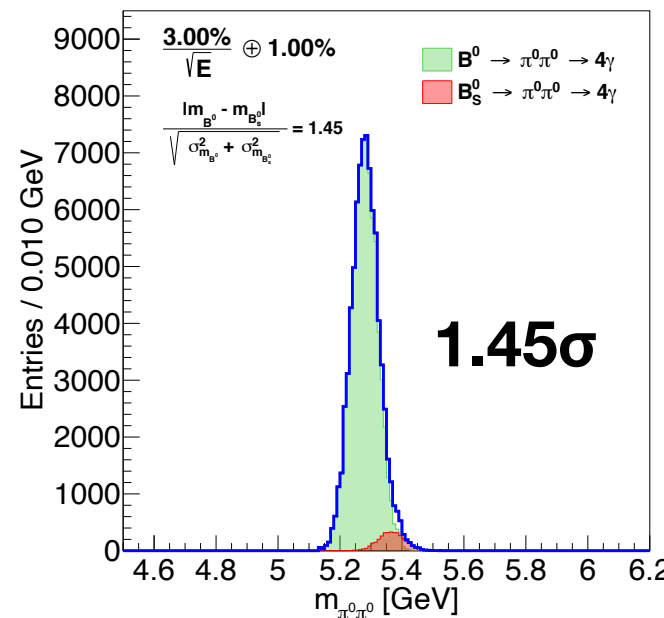
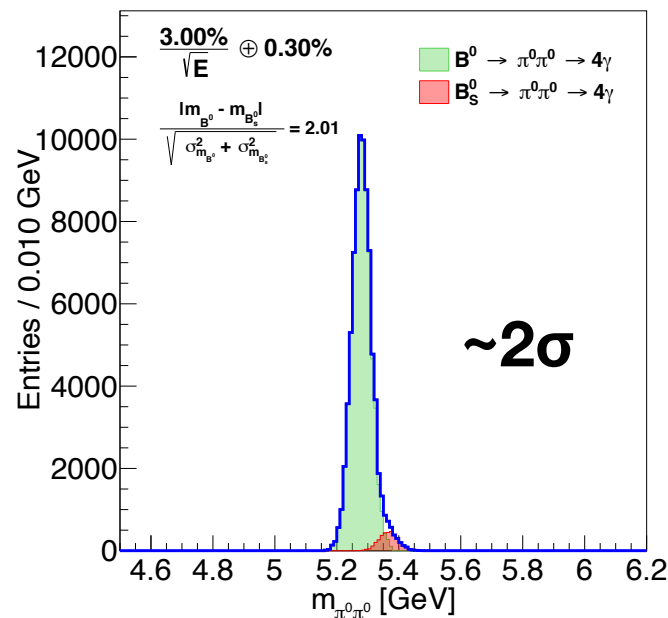
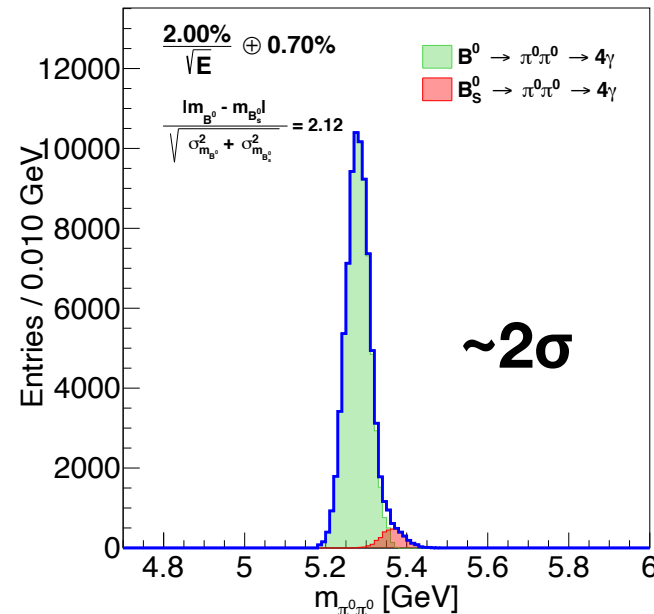
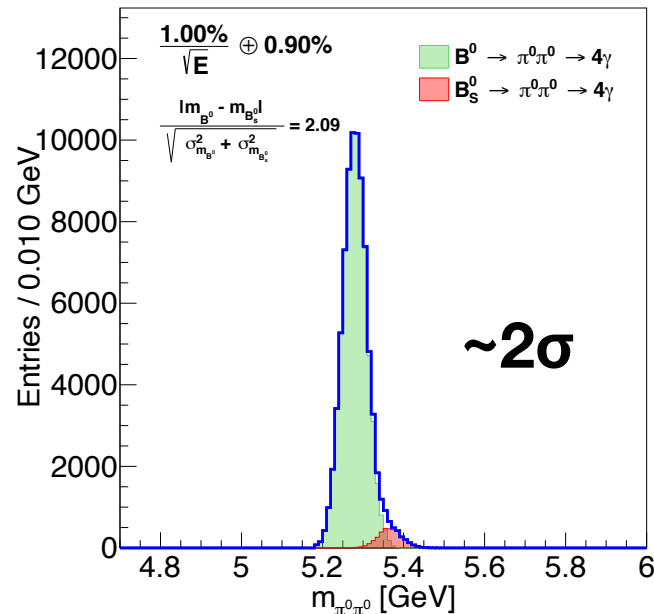
Leading kaon in B meson hemisphere



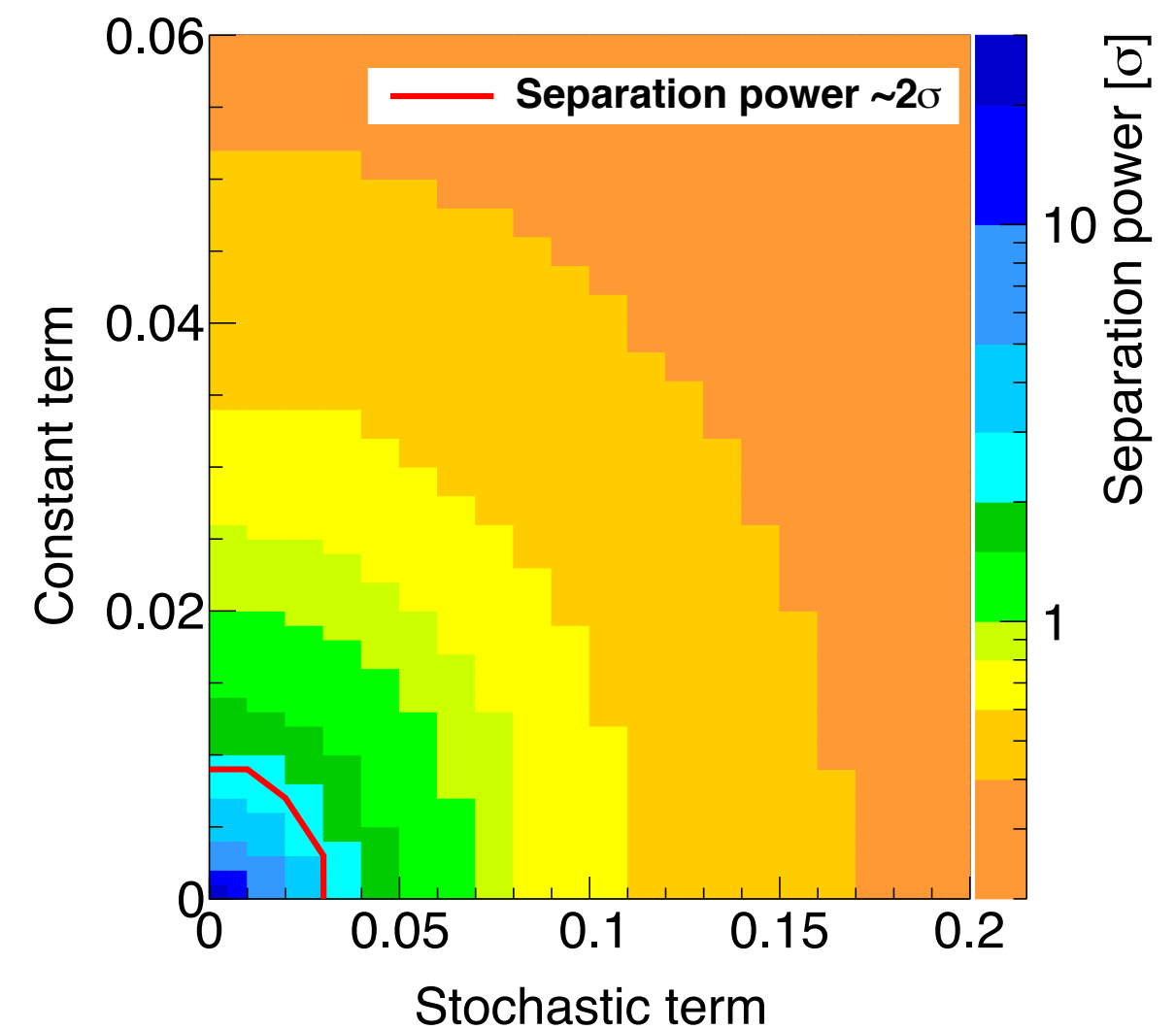
Separation of B^0 and B_s

$$m_{B^0} = 5279.63 \pm 0.15 MeV$$

$$m_{B_s^0} = 5366.89 \pm 0.19 MeV$$



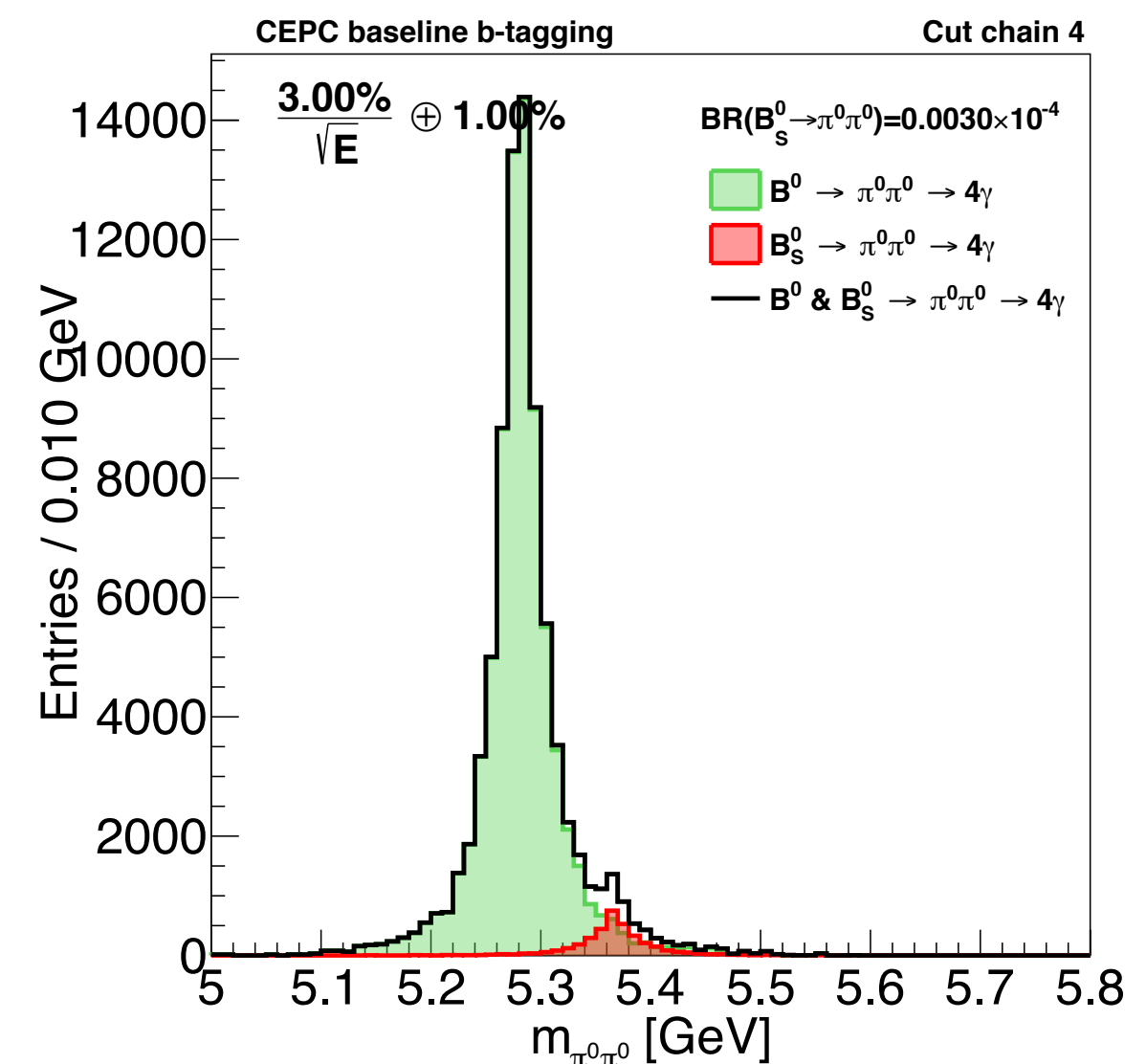
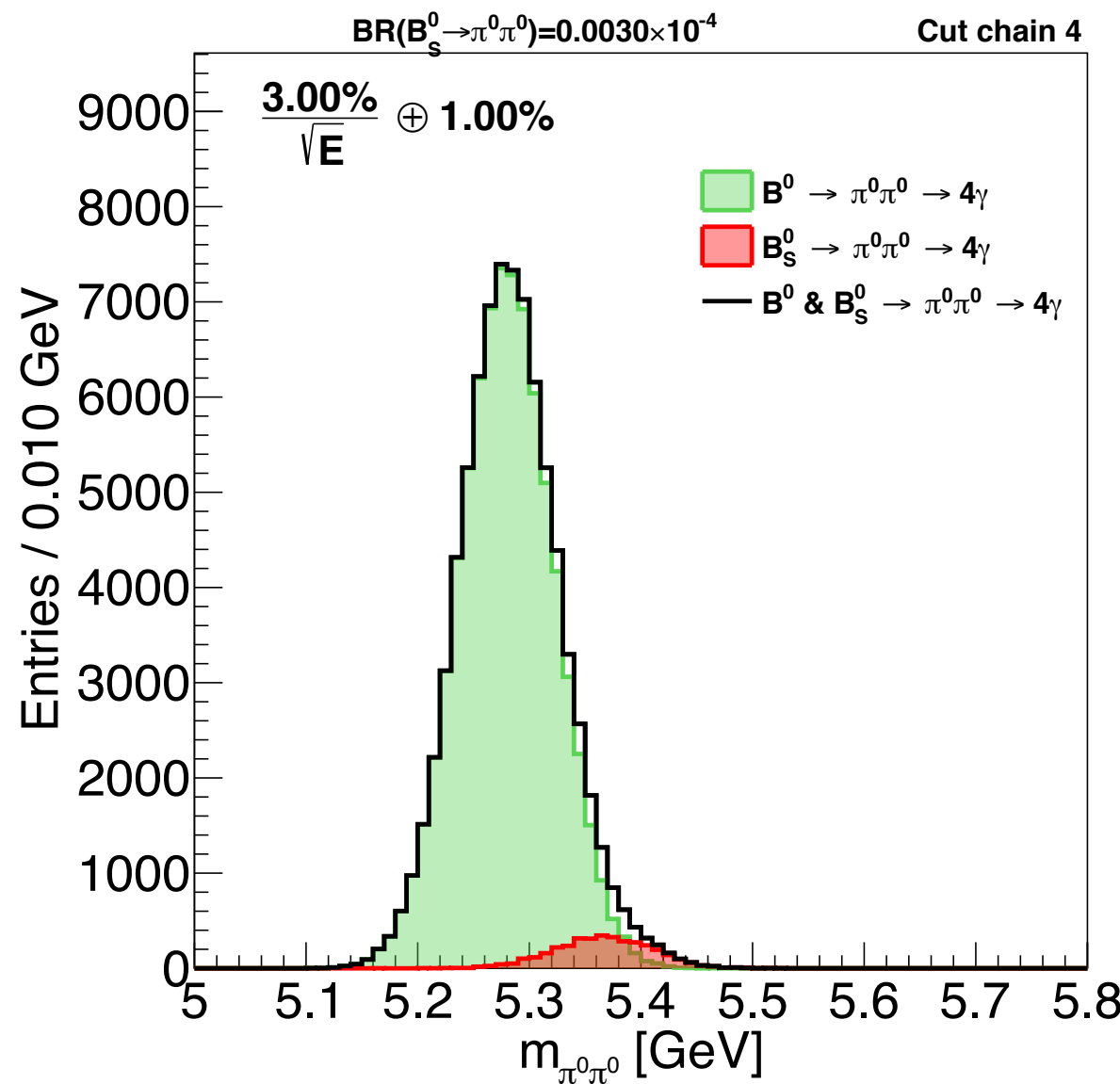
$$\text{separation power} = \frac{|m_{B^0} - m_{B_s^0}|}{\sqrt{\sigma_{m_{B^0}}^2 + \sigma_{m_{B_s^0}}^2}}$$



A 2σ separation requires ECAL energy resolution better than $3\%/\sqrt{E} \oplus 0.3\%$

Kinematic Fit

at $3\%/\sqrt{E} \oplus 1\%$ ECAL resolution



Signal peak gets sharpened after Kinematic Fit

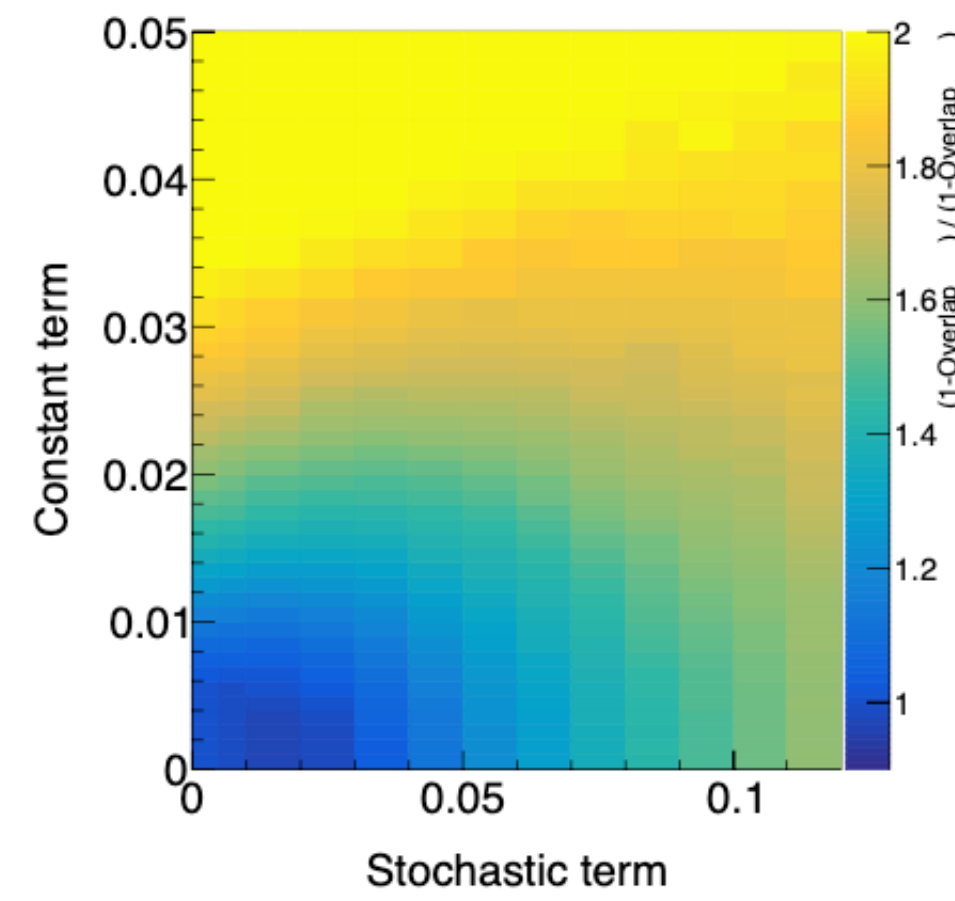
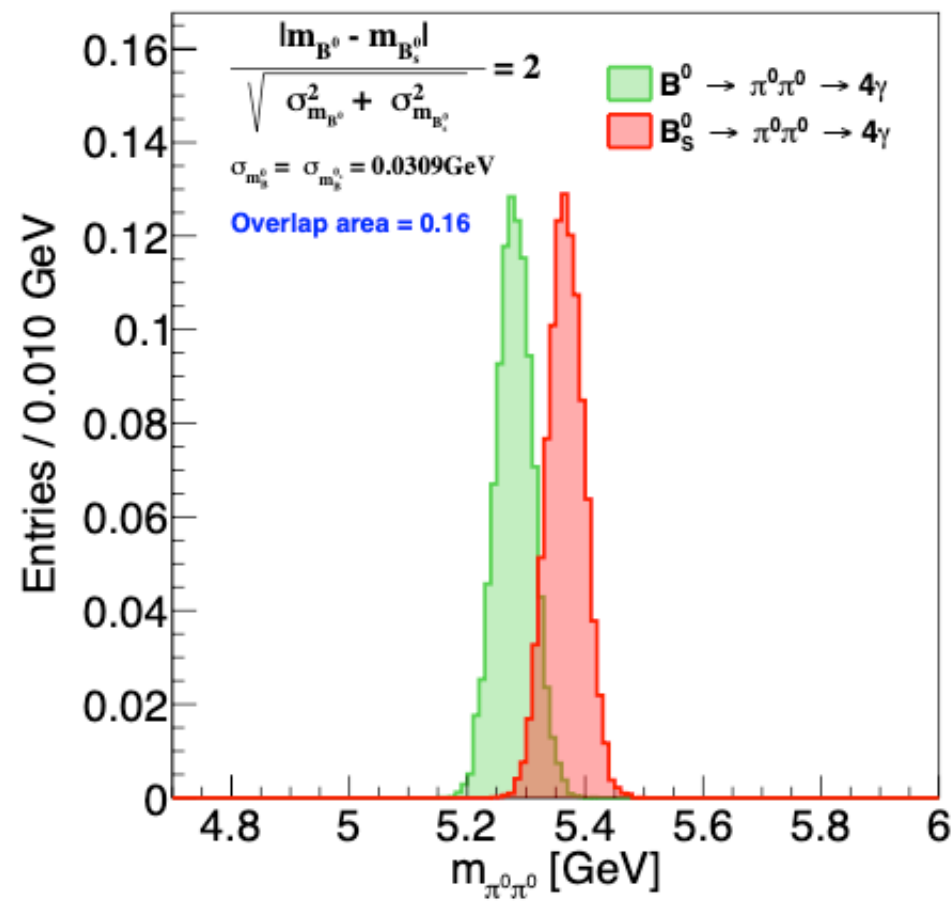
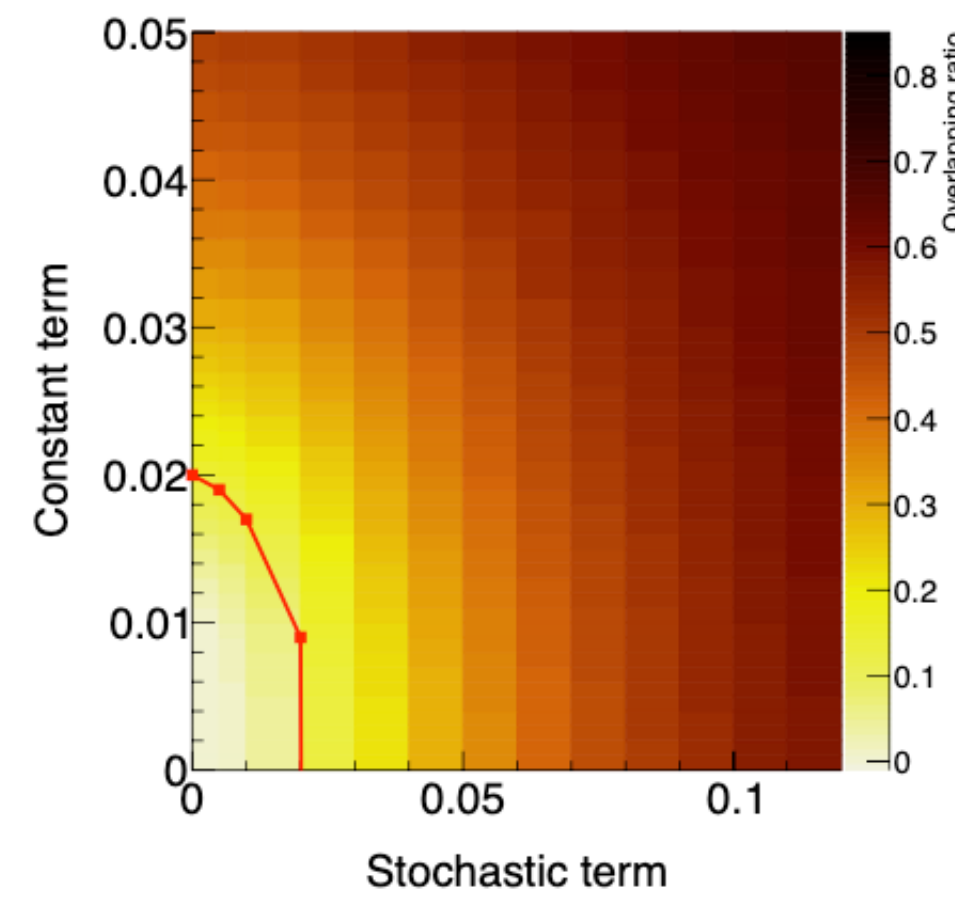
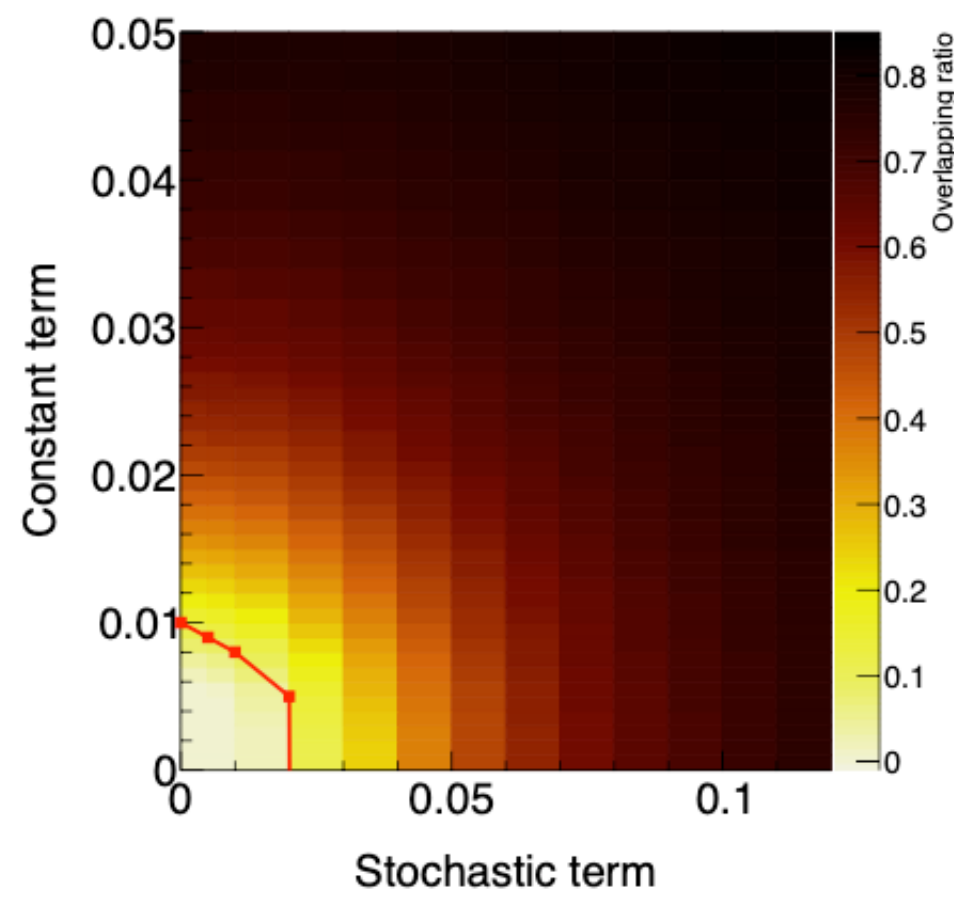


Figure 14: Separation power (overlapping area) at different ECAL resolutions wo/wi kinematic fit.